UPPSALA
UNIVERSITET

Digital Comprehensive Summaries of Uppsala Dissertations from the Faculty of Science and Technology 894

On Transfer of Work Material to Tools

JANNICA HEINRICHS

ACTA
UNIVERSITATIS
UPSALIENSIS
UPPSALA
2012

ISSN 1651-6214
ISBN 978-91-554-8261-9
urn:nbn:se:uu:diva-165828

Dissertation presented at Uppsala University to be publicly examined in Häggsalen, Lägerhyddsvägen 1, Uppsala. Friday, March 2, 2012 at 10:15 for the degree of Doctor of Philosophy. The examination will be conducted in Swedish.

Abstract
Heinrichs, J. 2012. On Transfer of Work Material to Tools. Acta Universitatis Uppsaliensis. *Digital Comprehensive Summaries of Uppsala Dissertations from the Faculty of Science and Technology* 894. 68 pp. Uppsala. ISBN 978-91-554-8261-9.

Bulk forming and cutting are widely used to shape metals in industrial production. Bulk forming is characterized by large strains, extensive plastic deformation and large surface expansions. Cutting is characterized by high speeds, high pressures and high temperatures. The prevailing conditions during these processes lead to transfer of work material to tools. In bulk forming this is a significant problem. The transferred work material is hardened and becomes harder than the work material, causing galling. This leads to high friction and high forming forces, bad surface finish of the formed products and significant difficulties to produce complicated geometries. In cutting, transfer of work material can be desired for protection of the tool surface. However, the transfer film has to be of the correct type to provide a stable and predictive behaviour during operation.

In this thesis the influence from tool material and surface treatment on work material transfer has been studied for both applications, with the use of simplified laboratory test methods followed by extensive surface studies. Both the tendency to, appearance of and chemical composition of work material transfer is evaluated. The results are compared with real industrial examples, to ensure that the correct mechanisms are mimicked.

In forming, the problems arise when poor lubrication prevails, due to high forming forces or large surface expansions. The transfer of work material can then be avoided with the use of a galling resistant coating, offering low adhesion. However, the coating has to be as smooth as possible, to avoid activation of the work material and subsequent transfer.

In cutting, the desired transfer film can be obtained by choosing the correct cutting parameters. The geometry and material of the fabricated component is often predetermined, setting the general cutting conditions, but the cutting speed influences the formation of the transfer film. Too low speed or too high speed leads to an unstable cutting process and poor surface finish of the piece. The speed intervals for each mechanism are partly determined by the tool material and thus by the tool coating.

Keywords: Tribology, Friction, Forming, Cutting, Galling, Material transfer, Tribological coatings, Surface finish, Micro mechanisms, Aluminium

Jannica Heinrichs, Uppsala University, Department of Engineering Sciences, Applied Materials Sciences, Box 534, SE-751 21 Uppsala, Sweden.

ISSN 1651-6214
ISBN 978-91-554-8261-9
urn:nbn:se:uu:diva-165828 (http://urn.kb.se/resolve?urn=urn:nbn:se:uu:diva-165828)

List of Papers

I *Laboratory test simulation of galling in cold forming of aluminium*, J. Heinrichs, S. Jacobson, Wear 267 (2009) 2278-2286

II *Laboratory test simulation of aluminium cold forming – influence from PVD tool coatings on the tendency to galling,* J. Heinrichs, S. Jacobson, Surface and Coatings Technology 204 (2010) 3606-3613

III *Mechanisms of transfer of aluminium to PVD coated forming tools,* J. Heinrichs, S. Jacobson, submitted to: Tribology Letters

IV *Evaluation of TiB_2 coatings in cold forming of aluminium,* J. Heinrichs, S. Jacobson, submitted to: Surface Engineering

V *The influence from shape and size of tool surface defects on the occurrence of galling in cold forming of aluminium,* J. Heinrichs, S. Jacobson, Wear 271 (2011) 2517-2524

VI *New understanding of the initiation of material transfer and transfer layer build-up in metal forming – In situ studies in the SEM,* J. Heinrichs, M. Olsson, S. Jacobson, submitted to: Wear

VII *Mechanisms of material transfer studied in situ in the SEM – Explanations to the success of DLC coated tools in aluminium forming,* J. Heinrichs, M. Olsson, S. Jacobson, submitted to: Wear

VIII *Evaluation of an intermittent sliding test for reproducing work material transfer in milling operations,* J. Gerth, J. Heinrichs, H. Nyberg, M. Larsson, U. Wiklund, submitted to: Tribology International

IX *Influence of sliding speed on modes of material transfer as steel slides against PVD tool coatings,* J. Heinrichs, J. Gerth, T. Thersleff, U. Bexell, M. Larsson, U. Wiklund, submitted to: Tribology International

X *Influence from surface roughness on steel transfer to PVD tool coatings in continuous and intermittent sliding contacts,* J. Heinrichs, J. Gerth, U. Bexell, M. Larsson, U. Wiklund, submitted to: Tribology International

Reprints were made with permission from the respective publishers.

The Author's Contribution to the Publications

Paper I	Major part of planning, experimental work, evaluation and writing.
Paper II	Major part of planning, experimental work, evaluation and writing.
Paper III	Major part of planning, experimental work, evaluation and writing.
Paper IV	Major part of planning, experimental work, evaluation and writing.
Paper V	Major part of planning, experimental work, evaluation and writing.
Paper VI	Part of planning, major part of experimental work, part of evaluation and writing.
Paper VII	Part of planning, major part of experimental work, part of evaluation and writing.
Paper VIII	Part of planning, experimental work, evaluation and writing.
Paper IX	Part of planning, major part of experimental work, part of evaluation and major part of writing.
Paper X	Part of planning, major part of experimental work, part of evaluation and major part of writing.

Contents

Introduction

Tribology is “the science and technology of interacting surfaces in relative motion and of related subjects and practices” [1]. It is described in terms of friction, wear and lubrication. Friction arises whenever two surfaces come into contact and experience relative motion, e.g. moves in different directions or with different speeds. The surface asperities of the opposite surfaces are going to contact each other and cause resistance against movement. Friction also arises when shearing a solid or a liquid. Where the conditions for friction prevail, wear can occur. The surfaces or surface asperities tear each other and if the local friction force overcomes the tensile strength of the weaker material, wear will result. Lubrication is used to reduce the problems caused by friction and wear. The lubricant ultimately separates the two solid surfaces, providing lower friction and less wear. However, several efficient lubricants are hazardous for the environment and are phased out. New environmentally friendly lubricants are introduced, but might not work as efficiently.

The surfaces are in any given moment decisive for the interactions taking place during sliding. However, the surfaces might not be very well described by the bulk material, but rather be an oxide, a deformation hardened layer or a layer of contaminants. With this said, the properties of the original surface might as well change with time, load, speed, deformation, environment, etc. Depending on the prevailing conditions, not just wear but also transfer of material from one surface to the other might occur. It could range from practically unaffected mating material to a tribofilm; a chemical reaction film formed in the tribological contact with differing composition and properties. This might cause problems, such as excessive wear or increased friction. It can also be a desired development and a prerequisite for the tribological system to work properly. In either way, the system has to be studied carefully as it changes and the resulting conditions have to be predicted to construct a well functioning tribological system.

To be able to predict the performance of a tribological system, highly detailed studies are necessary. The mechanical, chemical and physical properties of the uppermost surfaces, as well as the near surface regions, influence the tribological behaviour [1]. It can be expressed by parameters like hardness, material composition and melting point. The surface interactions can be measured and explained in terms of friction and wear. However, none of these descriptions take into account the appearance of the

contact, it is purely the effect of the contact. To obtain knowledge of what is actually happening, the surfaces have to be intimately studied, both before and after contact.

Aim of the thesis

The aim of this thesis is to investigate the mechanisms for transfer of work material to tools and to understand the conditions for transfer to occur. When the mechanisms are understood, precautions can be taken to avoid transfer of work material to forming tools, where this is a significant problem. With this understanding it is also possible to design the materials and cutting conditions for the desired tribofilm to form on cutting tools during operation, resulting in stable and predictive behaviour.

Metal forming

Metal forming is a group of efficient manufacturing methods, used in a number of industrial applications. They can be divided into sheet metal forming, exemplified by ironing, deep drawing and stamping, and bulk forming operations, exemplified by rolling, forging, extrusion and drawing. Bulk forming operations are characterized by very high strains and large forming speeds. They are generally fast and effective, with a low percentage of scrap material. The work pieces are formed in one or several operations, depending on complexity of the final product [2].

Forging and extrusion (of discrete parts) are two bulk forming methods with similar forming approach. They both comprise a tool consisting of at least two pieces, movable relative to each other. The work material billet is placed in the tool and the high pressure from closing the tool introduces compressive stresses in the billet, which plastically deforms into the new shape, defined by the tool pieces. An example, showing combined forward and backward extrusion, is shown in Fig. 1. Depending on the geometry of the billet and the formed product, the plastic deformation can be very high and the surface may expand several thousand percent [3, 4].

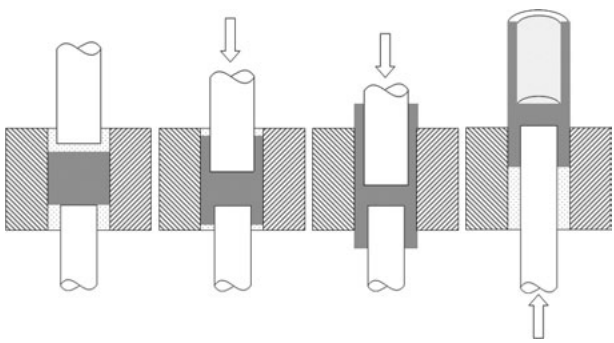

Figure 1. Sketch showing a bulk forming method, from billet to formed product.

High strength and low ductility of hardened materials make them difficult to form. A common solution is to form the alloy at an elevated temperature. However, where improved material properties or surface finish is required, the forging process is performed at ambient temperature, which does not influence the microstructure of the billet [2]. Another solution is to lower the strain rate, allowing a higher level of ductility, due to longer time for the

microstructure to respond to the deformation [5]. The product could then be formed in several steps with less deformation in each successive step.

During cold forging the surface expands in the direction of the deformation and virgin work material is exposed. The adhesion between the tool and work material is decisive for the subsequent course of events. If the adhesion is good, cold welding occurs. Continued sliding can then tear pieces out of the weaker work material, which continues to be welded to the tool surface [6]. If there is a lubricating film protecting the virgin work material and tool from contact, this can be prevented.

Galling

High stresses and high degree of plastic deformation during forming often lead to starved lubrication where the conditions are most severe. This leads to metal-metal contact and work material can be transferred to the tool [7], as mentioned in the previous section and exemplified in Fig. 2. The transferred material is then hardened by different hardening mechanisms, like grain refinement, work hardening and also by oxidation. When the next pieces are to be formed, the transferred material is harder than the fresh work material, which takes the shape of the tool now geometrically modified by the adhered material. The formed pieces can also be scratched by two body abrasion during the forming process. When the transferred material constitutes a significant amount, the surface finish of the products is compromised and the produced parts might no longer be within the tolerance limit. The transferred material then has to be removed, i.e. the tool has to be reconditioned. In aluminium forming, this is traditionally done by the use of NaOH, which attacks the aluminium to a higher degree compared to the traditionally used tool steels.

Figure 2. Photograph showing transferred work material on a punch after forming a number of aluminium products in production.

Galling occurs where the forming conditions are most severe, generally in areas with high degree of deformation, like in corners or when making thin walls. Also when precautions are taken regarding the geometry and severity of the forming, surface irregularities cause problems. Surface defects on tools, like grinding scratches and dents, act as traps for the work material. Local contact stresses are introduced and an even higher degree of deformation is reached and problem with lubrication is very likely to occur. These types of defects are believed to act as initiation sites for galling in sheet metal forming operations [8].

Lubrication in cold forming

Lubrication is used for several reasons in forming. It is of highest importance for the lubricant film to separate the work material from the tool to avoid adhesion and subsequent galling problems, as mentioned in the previous section. Lubrication is also used to decrease friction in the tool to work piece interface, to serve as a thermal barrier, if the work pieces are pre-heated (without influencing the microstructure), and to reduce tool wear [2, 3].

A lubricant to be used in cold forging has to be able to separate the tool from the fresh work piece material exposed during the great surface expansion. This implies that the lubricant needs good adhesion to one or both surfaces and great surface area increase to prevent galling [6]. The reaction with the newly exposed surface has to be fast so that a protective film is formed immediately. The newly exposed surface in aluminium forming is mainly aluminium since the aluminium oxide breaks at low loads, due to the difference in hardness. However, the importance of the lubricant also adhering to the aluminium oxide wear particles formed, to reduce wear, has been discussed [9]. Lubrication can also improve the quality of the product due to an improved deformation process. In addition, it can be desirable that the lubricant is easy to remove and that it is chemically stabile [10].

Proper lubricants in cold forging are metal coatings (e.g. easily shared tin or zinc), solid lubricants (e.g. graphite or molybdenum disulfide), polymer coatings deposited on the surface, liquid lubricants with proper additives and conversion coatings with additional lubricant [2]. However, while all of the mentioned lubricants might be sufficient for light-duty applications, the last mentioned lubricant system is the most commonly used and the only one sufficient for high strength aluminium alloys and the severe forming situations treated in this thesis.

A conversion coating is a porous reaction layer, closely adhered to the work piece surface, which acts as a lubricant carrier, see Fig. 3. Before this layer is formed, the surfaces are cleaned. Thereafter a zinc phosphate, calcium aluminate or aluminium fluoride conversion coating is applied by

soaking the aluminium work piece in a solution containing the necessary reactants. When the conversion coating has formed, a lubricant has to be added, since the conversion coatings offer no lubrication in themselves. Most commonly a solid alkaline soap film is used. The lubricant is mechanically trapped in the porous coating and can also be chemically bound to the coating [3]. Thus, the conversion coating offers a way to improve the adhesion between the lubricant and the work piece. The surface roughness can present lubricant reservoirs and since the conversion coating is closely adhered to the surface the probability to have lubricant present in the areas experiencing the most severe forming is increased. However, too rough surfaces or too thick lubricant films can result in insufficient surface finish of the formed product [2].

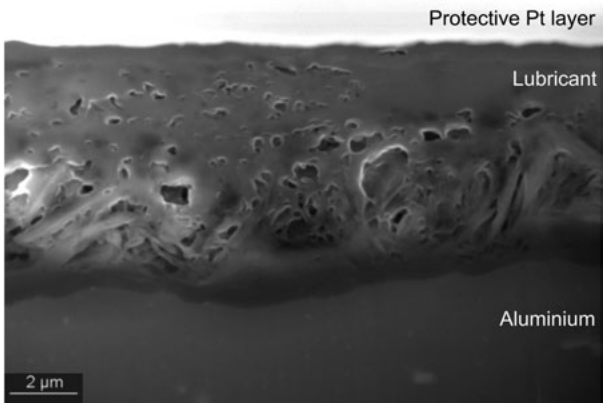

Figure 3. Lubricated aluminium work piece in cross-section. Imaged using SEM.

Metal cutting

Metal cutting includes a great variety of methods to shape metals. All these methods include a cutting edge, which cut into the work material and forms a chip while removing work material. The chip slides over the rake face of the tool, while the machined surface passes by the clearance face, also called the flank. The cutting tool is designed so that the flank is not in contact with the machined surface, to avoid high friction and poor surface finish [11], see Fig. 4. All processes are characterized by very high pressures and temperatures, placing extreme demands on the tool materials and making lubrication difficult [2]. Almost all metals can be machined, and with a great variety of work material properties follows a great variety of cutting conditions.

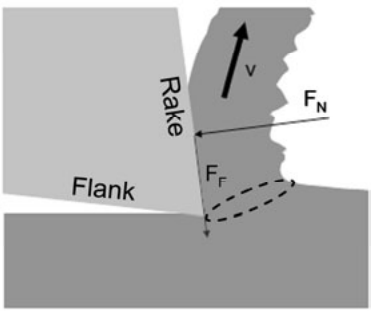

Figure 4. Sketch showing the contact between the cutting tool and the work material. The primary shear zone is indicated.

As the cutting proceeds, the work material surface and chip are heavily deformed and heat is generated in the primary shear zone (indicated in Fig. 4), in the secondary shear zone (along the interface between the rake face and the chip) and in the contact between the flank and the freshly cut surface if not adequately separated. Most of the heat is transported out of the contact by the chip, but some is also going into the presumably large work material piece and the small cutting tool. Although most of the heat goes elsewhere, the cutting tool usually becomes the warmest member in the system [12]. The warmest zone on the cutting tool is along the secondary shear zone, where the chip slides against the rake face [2]. At this position work material transfer is often found and in the continuation of the cutting

this zone is prone to wear. A higher cutting speed implies more heat generation and a warmer tool. If the temperature limit of the tool material is exceeded, the properties might change and rapid wear or fatal tool fractures can occur.

Too low cutting speeds can cause problems as well. Work material can be transferred and accumulated at the cutting edge, followed by strain-hardening of the transferred material. The accumulated work material then becomes harder than the work piece and, since it separates the tool from the work piece, it can act as the cutting edge, a so called built-up edge [11]. In the continuation of the cutting, the geometry and surface finish of the work piece might be undesired as the cutting edge geometry is altered and the built-up edge is unstable. Parts of or the complete built-up edge is continuously renewed and the removed fragments can leave the contact with the chip. This is not detrimental for the process as long as the tool stays intact. The fragments may also leave with the newly machined surface, leading to unacceptable surface finish of the product.

When the conditions are right, for the given combination of tool and work material, thin layers of transferred material could also function as an easily sheared barrier. It then protects the surface from wear as well as lowers the friction and the heat generation.

Turning

Turning is one of the most common metal cutting operations. The work material is a cylinder mounted in a lathe and rotated during cutting. The tool is stationary with a cutting edge that is pressed against the rotating cylinder, the motion that performs the cutting. The rate of removal depends on the depth of cut (the difference in diameter of the work material and the product). It is also dependent on the feed in the axial direction and the cutting speed. The cutting speed is usually set between 3 and 200 m/min, but in aluminium alloys it can be as high as 3 500 m/min [11].

The tool is in continuous contact with the work material during the cutting operation. To be able to comply with the heating of the contact, without opportunity to cool during the operation, the tool material needs to have high hardness, which is maintained at high temperatures. A low friction surface is also desired, to reduce the heat generation. A common solution is to have a substrate with high hot hardness and apply a top coating, which provides decreased friction and a wear resistant surface. As an example a Chemical Vapour Deposition (CVD) coated cemented carbide insert can be used, where the coating is decisive for the surface properties and the cemented carbide provides sufficient support for the coating.

Milling

Milling is another common cutting operation in industry. The tool usually has several cutting edges and is rotating performing the cutting operation. Each cutting edge experiences short term contacts with the work material, separated by periods out of contact, where it is unstressed and allowed to cool. This intermittent nature has a large influence on the tool, which suffers from both thermal and mechanical fatigue [11]. Here, cutting tools need higher toughness to deal with the repeated entrances and exits from the work piece, with the associated rapid variations in stress and edge temperatures, and could for example be made of Physical Vapour Deposition (PVD) coated High Speed Steel (HSS).

Materials

Aluminium

Aluminium is used in many applications due to its light weight, strength, corrosion resistance, workability, price and electrically as well as thermally conducting properties [13]. As soon as fresh aluminium is exposed to the atmosphere a native oxide, about 25 Å thick, forms a total coverage of the surface [14]. This oxide is dense, with good adhesion to the surface. The oxide is stabile and would always be expected on the aluminium surface in the pH range from pH 4 to pH 9. However, it is of much higher hardness than the aluminium (about 2000 HV in sintered condition [15] while aluminium alloys are typically less than 10 % of that), and is easily cracked when the aluminium is deformed.

To improve and design the properties for a specific application, alloying elements are added to the aluminium. Common alloying elements are silicon, iron, magnesium, manganese, copper and zinc [13]. High strength aluminium alloys achieve their strength through solution treatment followed by precipitation hardening. The alloys are divided into groups depending on their major alloying elements and thereby their properties.

Aluminium in the 6xxx-group contains magnesium and silicon as major alloying elements. During precipitation hardening Mg_2Si precipitates are formed, but also some Si particles. All 6xxx-alloys contain silicon in excess compared to the amount required to form stoichiometric Mg_2Si precipitates, to increase the age hardening response [16]. Also manganese and iron is to be found in these alloys, precipitating as AlFeMnSi and AlFeSi in the cell boundaries [17]. Manganese is also added to slow down recrystallisation and thereby control the grain size [18]. Among several alloys within the Al-Mg-Si system, AA6082 is considered a high strength alloy and is used where high tensile strength is needed. It is a very important alloy for industrial use, with the composition given in Table 1.

Table 1. Nominal composition of aluminium alloy 6082 (wt%). [17]

Si	**Mg**	**Mn**	**Fe**	**Cr**	**Cu**	**Zn**	**Others**	**Al**
1.2	0.78	0.50	0.33	0.14	0.08	0.05	0.15	bal

Case hardening steel

Case hardening steels are used in applications where a hard and wear resistant surface is needed, while the core should remain ductile and tough. This is achieved by having a ductile steel, which is more easily processed, and then harden the surface when in its final shape, while the core is practically unaffected. The base steel is often low in carbon content, less than 0.3 % [19], and to achieve intended hardening effect, the carbon and/or nitrogen content is increased in the surface by diffusion. Upon quenching, this introduce compressive stresses in the surface, and thereby hardness and wear resistance. Common applications are gears, where the gear teeth need the compressive stresses in the surface to avoid breakage when loaded. If the stresses turn to tensile, there is often tooth breakage at the root [20]. The steel used in this work, EN-ISO 20NiCrMo2 with the composition given in Table 2, is commonly used in gears.

Table 2. Chemical composition of EN-ISO 20NiCrMo2 (wt%).

Mn	**Ni**	**Cr**	**Si**	**Cu**	**C**	**Mo**	**Al**	**S**	**Sn**	**others**	**Fe**
0.86	0.58	0.55	0.24	0.21	0.20	0.18	0.039	0.013	0.012	0.03	bal

Tool steel

Tool steels are the group of steels that are used to form and machine other steels and materials. It is a large group of steels with different properties, since there are a wide variety of forming and machining operations. However, most of the tool steels are highly alloyed to meet the demands on wear resistance, strength and toughness in order to achieve optimum performance. There are several ways to group tool steels, for example according to alloy content, quenching method or application. In this section, three groups of steels are briefly described; cold work tool steels, hot work tool steels and high speed steels.

Cold work tool steels have been developed to provide very high wear and abrasion resistance in cold work applications. The required high hardness is achieved from high carbon containing martensite and finely dispersed carbides. The amount of alloying elements is decisive for the quenching method needed (low content requires oil quenching and high content might settle with air quenching) [21].

Hot work tool steels are designed to have high toughness to withstand impact loading, softening and thermal fatigue, when exposed to high temperatures. This is achieved with medium carbon contents, limiting the carbon content in the martensite making it less brittle, and with high

concentration of strong carbide forming elements, promoting toughness. The stable alloy carbides also improve resistance to softening [21].

High Speed Steels (HSS) are very highly alloyed in order to produce high densities of stable carbides. The large volume fraction of carbides increases the softening temperature remarkably. This makes this type of steel well suited for warm applications, like high-speed cutting and machining [22]. However, heated above its tempering temperature (usually above 500 °C [21]) they show thermal softening and the superior properties are lost. To protect the HSS against the high temperatures they are often coated in such applications.

Coatings

Coatings are used to modify the surface properties of a material without influencing the bulk material properties. By doing this, the specific material properties can be located where they are needed [23]. Coatings are mainly used in order to increase life time and performance of tools or products, by reducing wear, friction and/or adhesion in terms of adding hardness to the surface or decrease interacting forces etc. However, since the coatings are thin the substrate has to provide a sufficient support for the coating in order to avoid cracking of the coating.

There are several ways to deposit coatings, depending on coating material, substrate material, permitted cost, substrate geometry, coating thickness etc. Tool coatings in the micrometer range are usually deposited from a gas in a vacuum system by plasma-assisted techniques, since these can provide the adhesion and dense morphologies needed in tribological applications [23]. The two methods, which are by far the most common, are Chemical Vapour Deposition (CVD) and Physical Vapour Deposition (PVD). CVD is performed with gaseous reagents that react in the chamber and condense on the substrate to form the coating. CVD is generally performed at high temperature, 800-1200 °C, but it can be significantly lowered using plasma assisted CVD (PACVD) [23]. PVD involves evaporation of at least one reactant from a solid source inside the vacuum chamber. The resulting coating is the material of either the solid itself, the solid reacted with a gaseous reactant introduced into the chamber or a mixture of several solid sources and gases. PVD usually requires lower temperatures than CVD, typically from room temperature up to about 600 °C [24]. The temperature range for both methods limits the substrates to be used. CVD is mainly performed with ceramic substrates, like cemented carbide. Low-temperature CVD can be performed on HSS, but a subsequent heat treatment might be necessary if the temperature becomes too high. However, most steel substrates are coated using PVD.

Cutting tools are most often coated whereas forming tools are not. This is due to the large sizes and complex geometries of forming tools making it too expensive and complicated to apply coatings [24]. The large size of the tools also makes them expensive and a bad choice of coating could lead to coating detachment with coating fragments accelerating the wear of the tool. Also incorrect polishing of a rough substrate can lead to excessive removal of the coating and, in the worst cases, substrate break through. Polishing has to be done under controlled conditions, to remove the potential sources for material transfer initiation but not the coating in total [25]. However, when coated with a proper coating with sufficient surface finish, problems with transfer of material can be significantly reduced.

Cutting tools are commonly coated with hard coatings such as TiN, TiC and Al_2O_3 [23]. The coatings primarily provide a surface with high hardness, increasing the wear resistance, and as a consequence often decreasing the friction, thus reducing the heat generation. The coatings also function as a heat resistant temperature barrier against the heat generated, when shearing the work material and sliding against the chip.

Diamond-like Carbon

Diamond-like carbon (DLC) coatings are a group of mainly amorphous carbon based coatings with a wide variety of properties. The coating consists of both sp^2 (graphite-like) and sp^3 (diamond-like) hybridised carbon atoms in different relative proportions. The ratio between the two bonding types is decisive for the properties. A larger share of sp^2 bonds results in a more graphite-like type of coating and vice versa [26]. There are two clearly diverse groups of the material; hydrogenated and non-hydrogenated coatings. Except for carbon and hydrogen, additions of Si, F and N or metals like W, Ti, Nb and Ta are common and influence the properties [27]. The hardness is usually in the range of less than 10 GPa to 80 GPa, to be compared with 100 GPa for pure diamond [26].

Tribological test methods

To allow for simplified, fast and cheap tests out of production, a set of test methods have been used. The aim with each of them is to allow for studies of the critical part of the system, where unnecessary influences have been reduced and the actual problem is isolated. Thus, both tools and work pieces can be manufactured to simpler geometries, with higher control of the materials and surfaces, and easier interpretation of the results, due to direct correlation to measured friction, load etc. The equipments are used to screen materials and to study mechanisms, not for providing exact numbers for the industrial production.

Load scanner

The load scanner is a test equipment developed in Uppsala for evaluating galling [28, 29]. It comprises two crossed cylinders, one representing the tool and one representing the work piece. The tool piece slides over the work piece during increasing load and, with considerably softer work pieces, increasing degree of deformation, see Fig. 5. A longer sliding distance is achieved if the tool piece slides back during decreasing load. The strokes back and forth can be repeated as many times as wanted. The load increases and decreases in such a way that each part along the sliding path on the rod only experiences one load and has a unique tribological history [7, 30].

The normal load is applied by a spring, which is stretched during the motion of the sample, and monitored during the test duration. The friction force is continuously measured. The test interruption criterion can be modified depending on the critical limit for the system that is mimicked and can be e.g. a certain number of strokes, a maximum friction force, a maximum friction coefficient (calculated from the measured normal force, F_N, and friction force, F_T; $\mu = F_T / F_N$) or a maximum mean friction coefficient. The test has earlier proven very efficient for evaluating galling in cold forming [7].

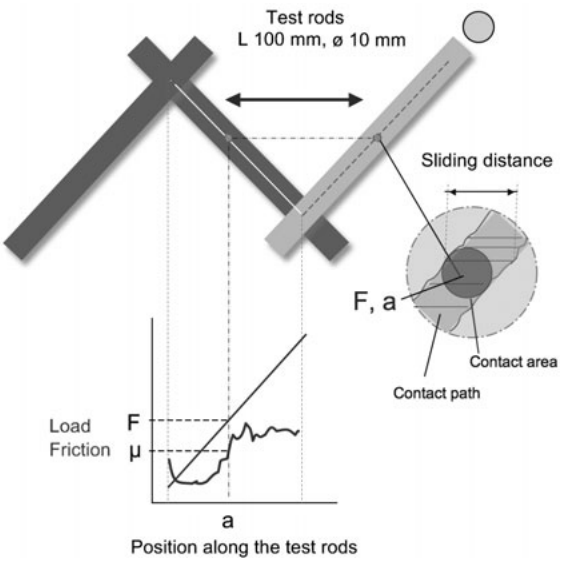

Figure 5. Sketch showing the principle and contact conditions in the load scanner.

In this work the test equipment has been used to evaluate galling resistance of tool materials against aluminium. With these conditions the contact pressure is practically constant in the whole load interval, and is decided by the hardness of the aluminium [30]. Instead the aluminium deforms plastically, the contact track gets wider and the sliding distance increases with increasing load, see Fig. 6.

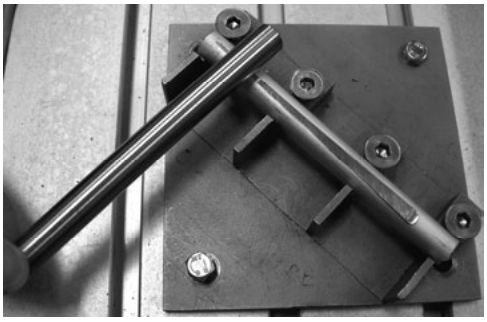

Figure 6. A test pair after sliding in the load scanner, experiencing increasing load. The tool steel cylinder is seen to the left and the aluminium cylinder to the right.

In situ sliding rig

The in situ sliding rig is a modification of the in situ manipulator, developed in Uppsala [31]. It is designed as a scratch tester, where a stationary diamond tip scratches a moving softer counter surface. The normal load on the tip is applied by a spring and is monitored during the test. The friction force is

measured while moving the counter surface. The in situ manipulator is designed to fit in an SEM, so that the influence from the diamond tip can be directly observed while running the test. The whole equipment is tilted 60°, to allow for direct observation with the electron beam, see Fig. 7.

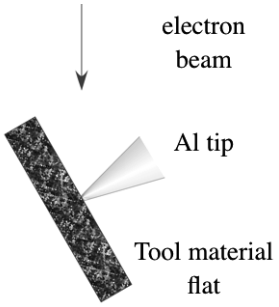

Figure 7. Sketch showing the principle of the in situ sliding rig in the SEM.

In this work the test equipment is modified to imitate galling in cold forming of aluminium. The diamond tip is exchanged for a tip of aluminium work material and the counter materials are selected tool materials. The tip is plastically deformed in the contact and the sliding distance is limited. Thus, the initial transfer mechanisms can be studied in a controlled environment and with knowledge about the very specific conditions in the contact.

Sliding contact rig

The sliding contact rig is constructed around a large turning lathe. It comprises two cylinders in sliding contact. One cylinder (diameter 0.14 m, length 1.0 m) represents the work material, and is placed as the rotating cylinder in the lathe. The other cylinder (diameter 5 mm, length 20 mm) represents the tool material and is pressed against the work material cylinder with a constant load by the use of a spring. The load and friction force is continuously measured using load cells. Fresh work material is introduced in the contact for each revolution due to the rotating motion and feed in the lateral direction, while the tool is in continuous contact with the work material [32], see Fig. 8.

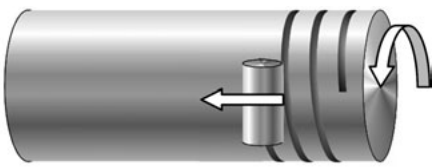

Figure 8. Sketch showing the contact conditions in the sliding contact rig.

Here, the sliding contact rig has been used to evaluate material transfer and wear for milling applications. To imitate milling, the sliding can be done intermittent, with enough time to cool the tool piece between the engagements. In traditional methods imitating cutting, the chip forming is included in the testing, which here can be excluded and only the sliding between the work material and the tool is imitated, to focus on transfer of work material and wear of the rake face. The load used is sufficiently large to deform the work material in the contact.

Analytical techniques

To evaluate the results from the tribological tests, surface analysis has been used extensively, both before and after tribological testing. The surface appearance, chemical composition and mechanical properties have been studied in several ways, depending on the purpose of the analysis. The most frequently used methods and instruments are briefly described in this section.

SEM

Scanning Electron Microscopy (SEM) has been used to image surfaces and cross-sections in high resolution. A variety of acceleration voltages have been used, to reach different imaging depths [33], and both back-scattered and secondary electrons have been used for imaging.

In this work cross-sections were imaged using a DualBeam FEI Strata DB235 with a Field Emission Gun (FEG). A Zeiss 1550 FEG SEM was used to image surfaces where high magnification, high resolution and low acceleration voltages were required (mainly in paper VI and VII). A complementary in-lens detector together with the FEG makes this instrument very suitable for studying thin transfer layers. A LEO 440 SEM with a LaB_6 filament was used to image surfaces and transfer films as well as for in situ galling studies. For complementary lower magnification studies and back-scatter imaging a Zeiss DSM 960A SEM with a W filament was utilized.

FIB

To be able to study the interfaces between coatings and substrates, transferred layers and tools and formed tribofilms on a tested surface cross-sections through these interfaces are needed. The latter two situations might present a very limited surface coverage and are thus unsuitable to prepare in the traditional way, with mechanical polishing, and hard to prepare without affecting the surface layers. Here, a Focused Ion Beam (FIB) instrument, FEI Strata DB235, was used to make cross-sections with micrometer precision positioning. The instrument compromises an SEM for imaging together with a focused ion beam, which is used for milling in the material to

make the cross-section. A protective film of platinum is deposited, using electron or ion beam assisted CVD, on the surface in two steps prior to milling, in order to preserve the surface. The initial platinum is deposited slowly using the electron beam and in the second step the ion beam is used, however with low current, for deposition of platinum at a higher rate. This instrument can also be used to produce electron transparent samples (less than 100 nm thick) and has a complementary manipulator arm, to be able to perform the lift-out technique [34].

TEM

To study transfer films with atomic resolution Transmission Electron Microscopy (TEM) was used. Appropriate areas were chosen, cut out and made electron transparent in the FIB, and then analysed using a FEI Tecnai F30 ST. The film as well as boundaries between work material and tool were imaged using Scanning TEM (STEM) and bright field imaging. Diffraction analysis was performed to determine crystalline phases in transferred films. For elemental mapping of the thin transfer films Energy Filtered TEM (EFTEM) was used. For a more comprehensive description on the techniques, see [35].

EDS

Energy Dispersive X-ray Spectroscopy (EDS) in an EDAX as well as Oxford Aztec X-max system have been used to prove the transfer of work material to tools and to analyse the chemical composition of transfer films. However, to get a reliable quantitative analysis, standard samples with a known chemical composition must be used to calibrate the system, as the probability for emitting an X-ray and for an emitted X-ray to reach the detector depends on the sample (atomic number, fluorescence tendency and absorption properties) [33]. Since the composition of the transfer films is varying and unknown on beforehand, no standards have been used and the analyses are only qualitative and not quantitative. The analysis depth is in the micrometer range and depends on acceleration voltage and sample. Relatively low acceleration voltages have been used where thin transfer films were to be analysed. However, the acceleration voltage has to be sufficiently high in order to excite the electrons in the elements to be analysed.

ESCA

Electron Spectroscopy for Chemical Analysis (ESCA), also known as X-ray Photoelectron Spectroscopy (XPS), has been used as a complement to EDS. ESCA is a surface sensitive method for chemical analysis at limited depth, where only the uppermost surface is analysed, up to 10 nm [36]. To analyse material further down from the surface a built in Ar^+ sputtering equipment has been used. With successive sputter removal of material from the top surface alternated with chemical analysis, depth profiles were recorded. Information about the chemical bonds has been derived as well. The recorded kinetic energy of the emitted electrons is element specific and dependent on the bonding energy of the electrons, causing an energy shift specific for the existing bonds.

The instrument used was a PHI Quantum 2000 with a monochromatic Al Kα X-ray source. It has mainly been used to characterize coatings and transferred material. Compositional changes in the films have been analysed by depth profiling. It has also been used as a method to detect transferred material, not visible in the SEM.

AES

To complement ESCA another surface sensitive method with higher lateral resolution was used, Auger Electron Spectroscopy (AES). The AES PHI 660 equipment was mainly used to analyse the chemical composition of transfer films covering a limited area. Instead of an X-ray source there is an electron gun illuminating the sample with electrons [37]. The electron beam is more focused than an X-ray beam, thus the higher lateral resolution. Besides that, the positioning is more exact, due to the higher resolution imaging possible with the electron beam. However, less information about the chemical bonds is derived, compared with ESCA.

White light interference profilometry

To record the topography of the surface, white light interference profilometry was performed on a WYKO NT 1100 equipment. It is a non contact optical measurement method based on the interference and reflectance of light [38]. It has a very high vertical resolution, down to nanometre range, and a lateral resolution in the micrometre range. The equipment was used to measure the surface topographies mainly before testing, to be able to compare surface characteristics of samples, and also after testing when applicable.

AFM

In order to describe surfaces with even higher resolution, Atomic Force Microscopy (AFM) was used. The method is based on interactions between a sharp tip and the sample. In non-contact mode, the two are never in contact. However, the sharp tip is fixed on an oscillating cantilever and the oscillation amplitude is influenced by the interacting force between the tip and the surface. As the sample is moved under the tip, the change in amplitude is monitored and the distance between the tip and the surface can be calculated. Thus, the surface topography can be described [39].

The instrument used in this thesis is a PSIA XE150 in non-contact mode. It has been used for describing extremely small surface protrusions in the nanometre range.

Nanoindentation

Nanoindentation has been performed using a CSM Ultra Nano Hardness Tester, equipped with a Nano Scratch Tester, for hardness measurements of coatings, transferred work material and for controlled introduction of small scale surface defects onto tools. A Berkovich diamond tip has been used for indentation and a spherically rounded diamond tip, radius 2 μm, for making scratches. The equipment is particularly suitable for mechanical tests in materials with limited thickness, as only small indentation depths are required. During indentation, load is linearly increased and the corresponding indentation depth is measured. From the load-displacement curve mechanical properties as hardness and elastic modulus can be calculated. Here, the calculations have been performed using the Oliver-Pharr method [40].

Contributions – on forming

Tool steel evaluation

Paper I

Aim

The purpose with this study was to evaluate different tool steels with regards to galling resistance. Previous studies have shown that a threshold surface finish is needed to resist galling, when it comes to forming of stainless steel [30, 41, 42]. To be able to observe the effect from chemistry also surface roughness was taken into account.

Experimental

Three tool steels, grade A, B and C, were evaluated in terms of galling resistance. Grade A is an ingot-cast conventional hot forming tool steel of matrix type with low content of carbides, Grade B is also an ingot-cast matrix tool steel, however modified to be suitable as a tough cold work tool steel, and Grade C is a nitrogen alloyed powder-metallurgical cold work tool steel with nominally 24 vol. % of carbides. Main alloying elements of the three steel grades are given in Table 3.

Cylinders (diameter 1 cm, length 10 cm) of the three steel grades were prepared to two surface roughnesses, ground to Ra 0.3 μm and polished to Ra 0.02-0.04 μm. All grades were tested against unlubricated as well as soft annealed and lubricated aluminium AA6082, to compare their galling resistance, in the load scanner equipment. The tests were performed by single strokes as well as multiple passages, with a sliding velocity of 0.01 m/s for a single stroke and 0.02 m/s for multiple passages and a load interval of 100-1200 N. The threshold for severe galling, thus the interruption criterion, was set to a friction force rising to or above 1000 N.

Table 3. Main alloying elements of the tested tool steels grades, provided by the steel manufacturer (wt%).

Grade	C	Si	Mn	Cr	Mo	V	W	N
A	0.4	1.0	0.4	5.2	1.4	0.9	-	-
B	0.5	0.2	0.5	5.0	2.3	0.5	-	-
C	1.1	0.5	0.4	4.5	3.2	8.5	3.7	1.8

Results and discussion

The friction coefficient during the single strokes test was of the same magnitude, irrespective of tool steel grade and surface finish tested. However, the aluminium pre-treatment gave a completely different behaviour. Unlubricated tests gave a friction coefficient of about 0.8, while the addition of a solid lubricant decreased the friction coefficient to about 0.2. Almost all unlubricated tests reached the interruption criterion already during a single stroke (corresponding to 0.5 passages), see Table 4.

Table 4. Maximum number of passages back and forth until the friction force threshold ($F_T \geq 1000$ N) was reached.

Grade		**Aluminium**	
		Lubricated	Unlubricated
A	Ground	33.5	1.5
	Polished	40.5	0.5
B	Ground	37.5	0.5
	Polished	34.5	1.5
C	Ground	28.5	0.5
	Polished	34.5	0.5

The friction coefficient development showed some differences between ground and polished surfaces. With ground surfaces, the friction coefficient showed a slow but continuous increase. With polished surfaces, the friction coefficient was steady for about 20 passages back and forth, and thereafter it rapidly increased until the friction force threshold was met, see Fig. 9.

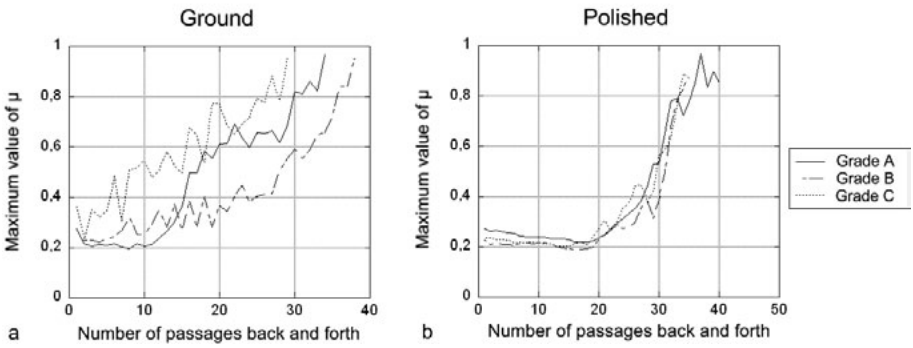

Figure 9. Maximum coefficient of friction in each individual passage against lubricated aluminium. The test was interrupted when the friction force grew higher than 1000 N. Testing was performed with a) ground tool rods and b) polished tool rods.

With the rougher surfaces the lubricant was stored in scratches and could be portioned out during the test. The friction coefficient increased, due to transfer of aluminium to the scratches, but at a lower rate than in the smooth

case. With the polished tool surfaces the lubricant film was sheared and decided the friction coefficient. However, the lubricant was transported to the rims of the contact, due to the high pressures, and eventually there was starved lubrication in the contact and friction rose rapidly. The result was that tests with both surface finishes reached the friction force threshold after the same number of passages, but for different reasons, see Fig. 9 and Table 4.

All tool steel grades of the same surface finish showed a similar appearance of the contact track. Thick transfer layers of aluminium were mainly transferred in connection to grinding scratches, see Fig. 10. Also in absence of visible scratches on the polished tool steel rods, aluminium was transferred, in thinner layers, to the polished tool surface, see Fig. 11.

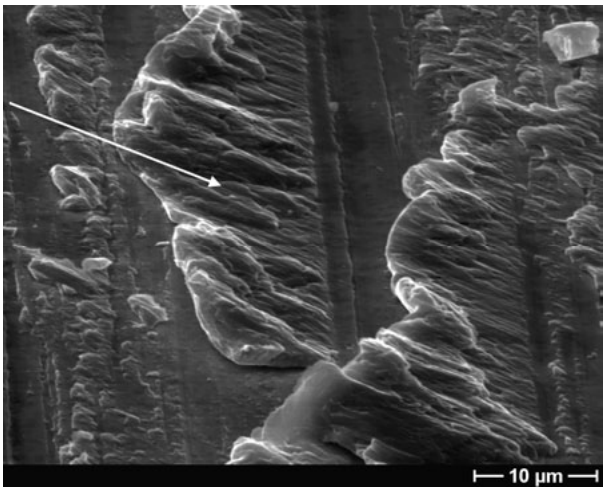

Figure 10. Transferred aluminium was mainly found in connection to scratches on the ground surfaces. Here, ground tool steel grade C after a single stroke against unlubricated aluminium. The arrow indicates the sliding direction.

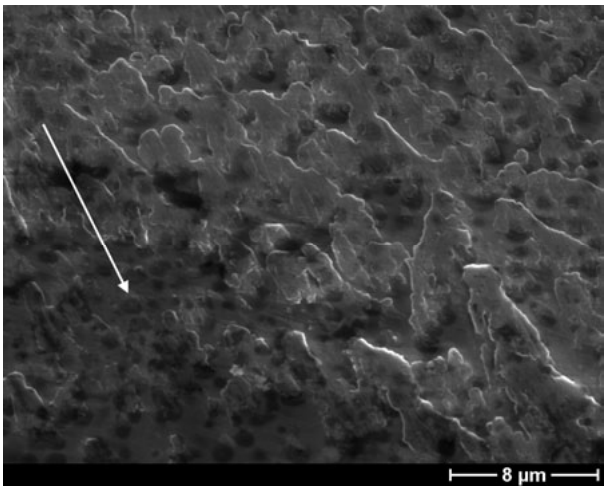

Figure 11. On the polished tool steel surfaces, in absence of visible scratches, aluminium adhered to the polished surface as well. Here, polished tool steel grade C after a single stroke against unlubricated aluminium. The arrow indicates the sliding direction.

Main conclusions

All tool materials exhibited the same severe galling mechanism and could not be distinguished with respect to amount of transferred material. Galling occurred in correlation to scratches but also on the smooth surface. The lubricant turned out to be of very high importance, since not even the smoothest tool surfaces (Ra = 0.02–0.04 µm) could avoid immediate transfer of aluminium from the unlubricated aluminium cylinder. Lubricant significantly decreased friction and increased tool life.

Tool coating and surface preparation

Paper II, III and IV

Aim

Since the lubricant turned out to be of highest importance to avoid galling, it is detrimental to have lubricant film break-through. This is however the case in many forming operations, with high stresses and surface expansions. Addition of a coating to the forming tool is one way to avoid direct aluminium to tool steel contact. The aim of these studies was to evaluate possible coating materials with regards to galling resistance, against aluminium in lubricated and unlubricated condition.

Experimental

Nine coatings were tested in the load scanner against unlubricated as well as soft annealed and lubricated aluminium AA6082 to compare their galling resistance. Tool steel grade A from the previous section was used as substrate and an uncoated reference. Coating type and technical data is found in Table 5.

Table 5. Test material No., type and technical data, as given by the coating manufacturers. Coating No. 10 is a non-commercial coating produced by the author.

No.	Coating (+ indicates a top layer)	Deposition method	Hardness [HV]
1	Uncoated tool steel	-	510
2	a-C:H:Me + a-C:H	PVD sputtering + PACVD	1000-1500 + 2000-3000
3	a-C:Me	PVD sputtering	800-1200
4	TiAlN + a-C:Me	PVD arc + PVD sputtering	3000-3500 + 800-1200
5	TiAlN	PVD arc	3000-3500
6	TiAlN + a-C:H:Me	PVD arc + PVD sputtering	3000-3500 + 1000-1500
7	TiN	PVD arc	2000-2500
8	TiAlN	PVD arc	3000-3500
9	TiCN + a-C:H:Me	PVD thermal evap + PVD sputtering	2800-3200
10	TiB_2	PVD sputtering	3000-3800

The tests were performed with single as well as multiple strokes, with a sliding velocity of 0.02 m/s and a load interval of 100-1000 N. The threshold for severe galling was set to a threshold friction force of 1000 N. For the lubricated tests a complementary limit of 200 strokes was used, due to considerable plastic deformation of the soft annealed aluminium also in the contact with the sample holder.

A new load scanner equipment was employed when testing coating No. 10. A modified galling criterion could then be used. Instead of a maximum friction coefficient a mean friction coefficient value, calculated for the most recent passage back and forth, could be used as an interruption criterion. This is actually a better galling estimation, as it takes the total amount of aluminium in the contact track into account, and not just the worst situation in the track. As soon as this value grew higher than 0.5, the test was interrupted. The load interval was also adjusted to 50-800 N, due to technical reasons. In the following text coating No. 10 will still be presented together with material No. 1-9, since the comparison with uncoated tool steel, tested with both equipments, turned out similar.

All tool materials were prepared to two surface roughnesses to enable evaluation of the chemistry without influence from too rough surfaces. The surface roughness parameters are found in Table 6.

Table 6. Surface roughness parameters, in µm, of the rougher tool rods, R, and the smoother tool rods, S, as measured with white light interference profilometry.

Designation	**1R**	**2R**	**3R**	**4R**	**5R**	**6R**	**7R**	**8R**	**9R**	**10R**
Ra mean	0.17	0.13	0.15	0.18	0.36	0.21	0.21	0.20	0.22	0.29
Rt mean	2.4	2.0	2.1	2.8	4.7	4.3	2.7	3.0	3.9	3.2
Rpk mean	0.20	0.13	0.12	0.22	0.37	0.40	0.26	0.26	0.48	0.29
Rvk mean	0.24	0.25	0.22	0.28	0.43	0.29	0.24	0.29	0.30	0.41
Designation	**1S**	**2S**	**3S**	**4S**	**5S**	**6S**	**7S**	**8S**	**9S**	**10S**
Ra mean	0.026	0.042	0.041	0.055	0.038	0.068	0.036	0.043	0.054	0.032
Rt mean	0.31	1.4	2.5	1.6	1.7	3.1	0.47	1.8	2.6	0.46
Rpk mean	0.018	0.095	0.053	0.14	0.029	0.076	0.030	0.050	0.059	0.041
Rvk mean	0.032	0.059	0.064	0.15	0.11	0.28	0.062	0.11	0.15	0.053

Results and discussion

The maximum number of strokes to reach the pre-determined friction criterion proved to depend on lubrication, tool surface roughness and type of coating. When performing the tests lubricated, some of the rods reached the test limit of 200 strokes and the worst performing coatings reached about 80 strokes, which correspond closely to the performance of the uncoated rods, see Fig. 12. The difference between ground and polished tool rods was, in most cases, limited.

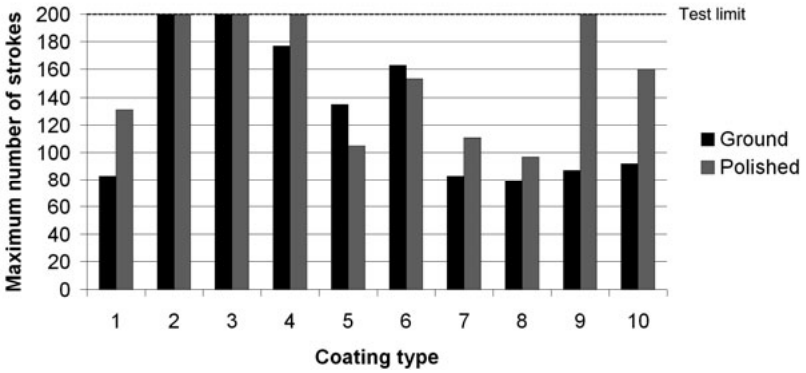

Figure 12. Maximum number of strokes against lubricated aluminium before the friction force threshold of 1000 N was reached. The test was interrupted after 200 strokes if the friction threshold was not already met.

When forming the unlubricated aluminium, all rough coatings failed within 13 strokes or less, see Fig. 13a. Polishing improved the performance of all coating materials, but not to the same extent. The best coatings, No. 2 and 3, performed well for more than 1000 strokes in polished condition, see Fig. 13b. Coating No. 4 also performed significantly better than 5-10, with more

than 300 strokes. The rest of the coatings as well as the uncoated reference reached the threshold in less than 20 strokes, also in polished condition.

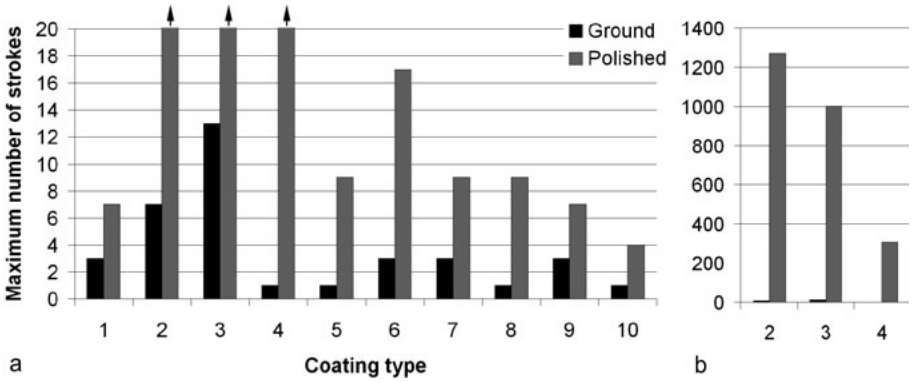

Figure 13. Maximum number of strokes against unlubricated aluminium before the friction force threshold of 1000 N is reached. Showing a) the first 20 strokes and b) coating No. 2-4 in full scale.

The friction increased in one or several spots along the contact track until the friction force threshold was reached. A comparison between the friction results and images of the contact tracks after lubricated tests showed that the high friction peaks in the friction graphs corresponded closely to areas covered by aluminium in the contact tracks, see Fig. 14. Polished samples showed transferred material preferably in the higher load region, corresponding to longer sliding distances. With the rough samples, aluminium was transferred to almost the entire track, and friction grew high during the full stroke, see Fig. 14b. This was valid also for rough samples tested without lubricant. The polished coating areas covered by adhered material showed no accumulation of defects or scratches, when studied in cross-section. Neither was there coating detachment or damage of the coating.

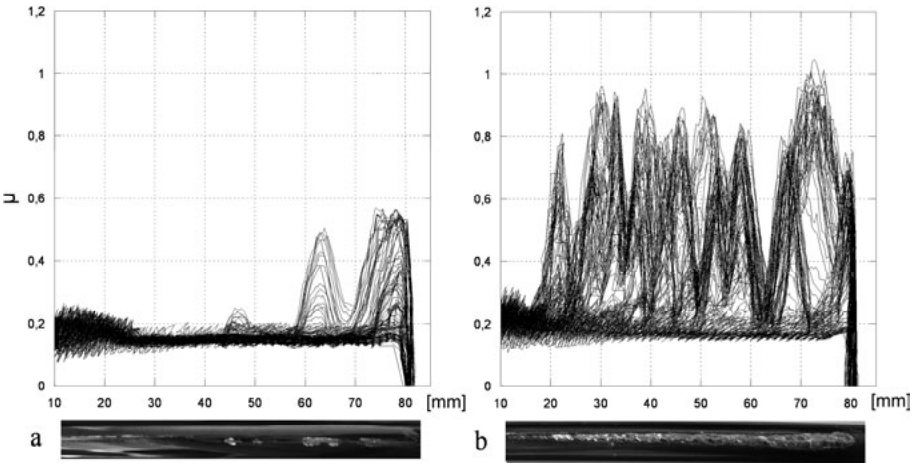

Figure 14. Friction development curves and corresponding contact tracks from lubricated tests. Load increases to the right. a) Polished coating No. 3 after 200 strokes and b) ground coating No. 3 after 200 strokes.

If the work material side was studied more closely after lubricated tests, the contact track on the cylinders from tests interrupted before the threshold friction force was reached showed different shaded areas, see Fig. 15. The dark grey areas, corresponding to areas where transfer to the tool was limited, were covered by a tribofilm and light grey areas, corresponding to areas with extensive transfer, were bare. Chemical analysis of these areas confirmed that the tribofilm, where present, consisted of lubricant, aluminium and aluminium oxide, while the bare areas had the same composition as the aluminium alloy.

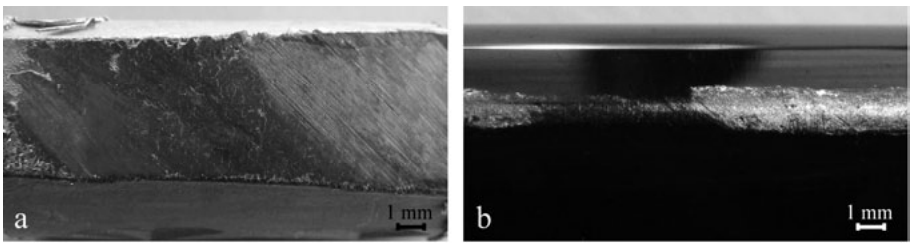

Figure 15. Top view images showing a) darker grey and lighter grey areas in the contact track on a lubricated aluminium rod tested against a smooth coating No. 3 and b) the corresponding part of the contact track on the smooth coating No. 3.

These areas on the work material were further studied in cross-section using FIB. The bare areas showed a few pores in the cross-section, but very little difference between the outermost layers and further down, see Fig. 16a. The tribofilm showed a strong mixing of the surface near layers, to a depth of several micrometres, see Fig. 16b.

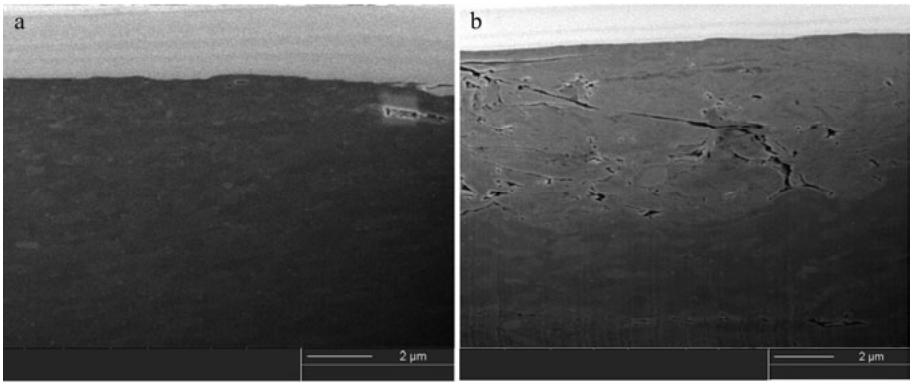

Figure 16. Cross-section images of the contact track on lubricated aluminium tested 200 strokes against polished coating No. 3. a) Bare area and b) area with tribofilm.

The tribofilm seems to prevent galling, but was loosely adhered to the work material and probably gradually removed. When there was no tribofilm separating the surfaces, aluminium was transferred to the tool an eventually galling occurred.

In the unlubricated tests, the explanation for galling preventing properties is not as straight on. Although the importance of smooth surfaces was evident from Fig. 13, it was not the only explanation. The polished uncoated tool steel showed the smoothest surface of all samples, but did not prevent galling. Some of the coatings were as smooth as or smoother than coating No. 2 and 3, but did still cause galling. Coating No. 4 seems to be one of the roughest coatings after polishing, but still performed better than coating 5-10 and the uncoated reference. This means that the surface chemistry is decisive. However, when the surface chemistry was favourable, small differences in roughness became important. The composition of the top layer on No. 4 was the same as on No. 3, but with a rougher surface. This shows as a 70 % decrease in tool life with the criterion used here.

The most favourable chemistry is not that easy to define. The best performing coatings were all of DLC type, however so was also coatings No. 6 and 9, which did not show any superior behaviour. Neither the hardness was the clue to successful coatings, with a wide range of hardness values in both successful and galling prone coatings. However, coating No. 2 and 3 from this work showed low adhesion towards the aluminium work material and are good candidates for aluminium cold forming applications.

Main conclusions

A surface with good galling resistance should keep lubricant in the contact, by facilitating formation of a tribofilm, and delay galling even if the lubricant layer becomes very thin or is locally missing. In these respects, DLC coating No. 2 and 3 excels, No. 4 is quite good, while the others are just slightly better or similar to the uncoated tool steel. However, the coating

surface needs to be very smooth, none of the tested coatings can help in the case of insufficient lubrication and rough tool surfaces.

Influence of local defects

Paper V

Aim

Since surface roughness proved to have a decisive role when preventing galling, a surface roughness limit is interesting to find. The aim of this investigation was to find a threshold roughness or defect size that causes galling.

Experimental

To find a threshold surface roughness for galling prevention, different degrees of surface roughness were introduced to a galling resistant surface. This was done by starting with a fine polished coating with a favourable surface chemistry, coating No. 2 from the previous section. Subsequently, surface defects were introduced to the surface in a controlled manner, by use of nanoindentation, microindentation and scratching with SiC grinding paper. Groups of indents were made along the coated cylinder with a separation of 8 mm and a depth of 8 nm, 65 nm, 160 nm, 650 nm, 1.5 μm and 5.6 μm, one depth on each rod. A less controlled type of irregularities was made by scratching the coating in 3 mm wide bands with SiC grinding paper using a load of 1.5 N and alternating the grit sizes 1000 (0.7 μm wide scratches), 500 (1.5 μm wide) and 240 (9 μm wide scratches plus coating fracture), in that order. The positions of the bands corresponded to the loads of 65-180 N, 460-655 N and 770-950 N in the contact track. A fine polished surface (Ra 0.03 μm) as well as a ground surface (Ra 0.1 μm) were tested as references. Tests were performed unlubricated in the load scanner test equipment with the aluminium alloy AA6082 as work material. The load interval was set to 20-1000 N and the interruption criterion was set to a maximum friction force of 1000 N or extensive wear of the aluminium cylinder.

Results and discussion

The introduction of surface defects did not significantly affect the friction during the first stroke, see Fig. 17. Only the ground tool showed a clearly higher friction.

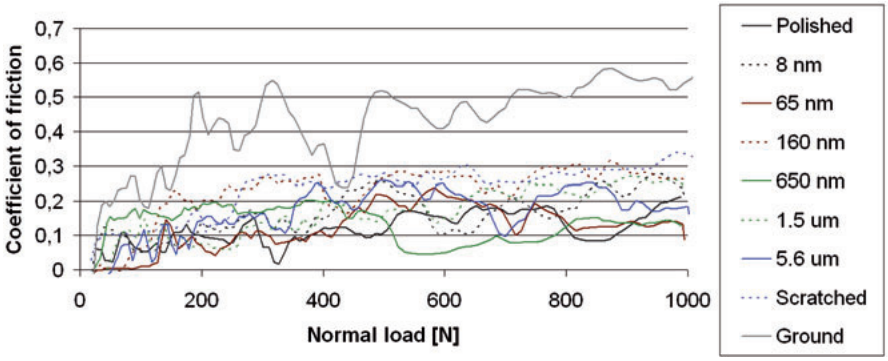

Figure 17. Friction coefficient during the first stroke between the different tool rods and an aluminium rod.

However, studying the contact tracks of the tool specimens showed that aluminium has transferred to the occasional indents and to a much greater extent than to the surrounding polished surface, see Fig. 18.

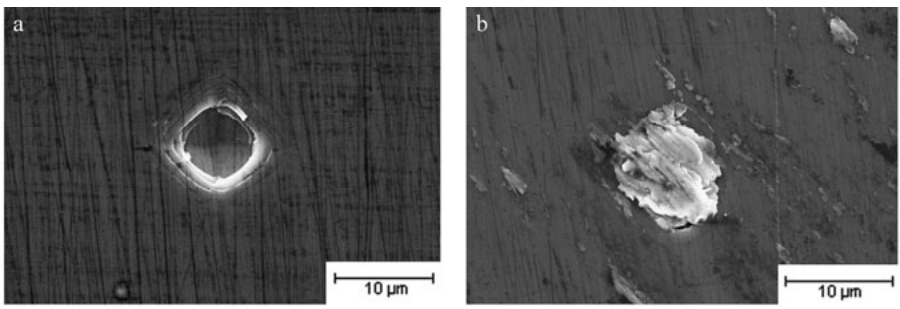

Figure 18. SEM images of a 1.5 µm indent at the position with corresponding load 100 N a) before and b) after one stroke against aluminium.

The occasional indents did not have any influence on the friction coefficient development, compare Figs. 19a and b. However, the small occasional indents did not cover a large fraction of the contact track area and even though aluminium was indeed transferred to the indents to a high degree, the associated high local friction did not contribute significantly to the total friction level. The rod scratched with SiC paper distinguished itself, by an increased friction at high loads. A high friction plateau was formed after 300 strokes and above 500 N and maintained throughout the test, see Fig. 19c. These scratches affected a larger area of the contact track and the fraction seems large enough to significantly influence the total friction. The ground tool rod showed high friction already from the start and the threshold friction force was met and the test interrupted, see Fig. 19d.

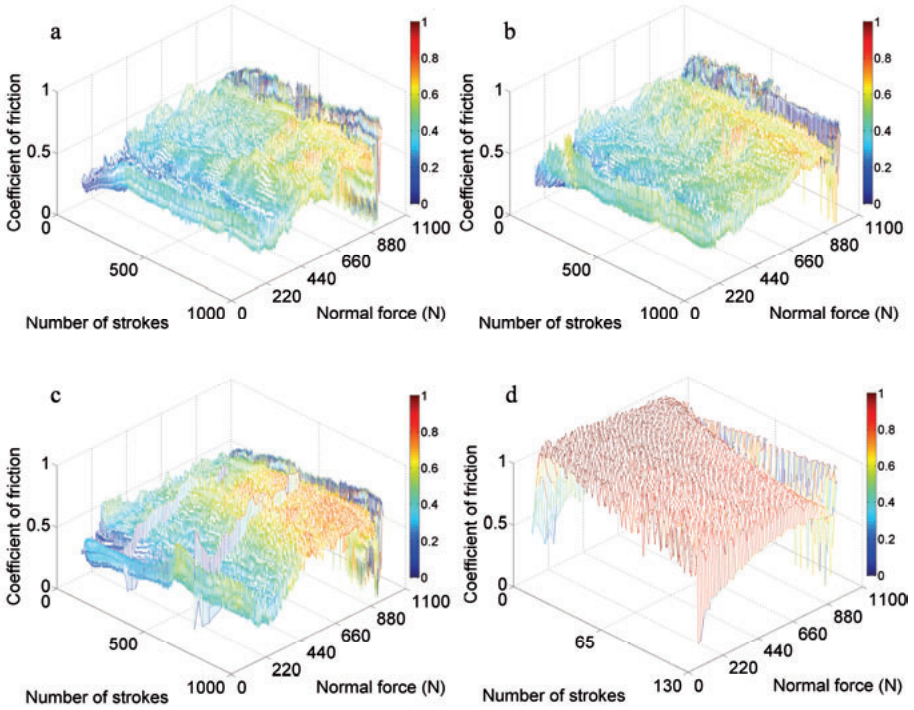

Figure 19. Friction coefficient development of the test with aluminium against a tool rod with a) polished surface, b) 5.6 µm indents, c) scratches and d) ground surface. (Notice the difference in number of strokes.)

However, the friction showed a tendency to increase with number of strokes also for the polished specimen, irrespective of presence of indents. This was due to aluminium being transferred to the polished surface on the fine polished rod as well as the area surrounding the indents on the indented rods, see Fig. 20. The indents were barely visible.

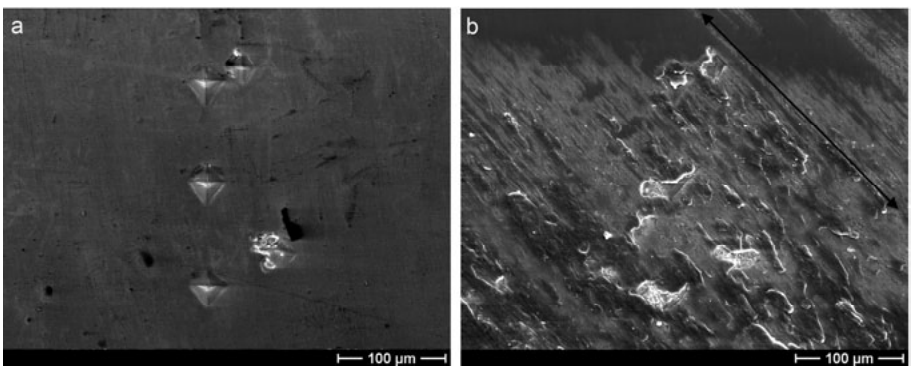

Figure 20. SEM images of an indented tool rod at the position which has experienced a load of 360 N. a) Before and b) after multiple strokes against aluminium.

Cross-sections of indented tool rods after testing showed that the indents were filled with aluminium already after the first stroke, see Fig. 21a. Additional strokes lead to transfer to the polished surface in general, but not to build-up from the material in the indents, see Fig. 21b. However, the aluminium in the indents increased in hardness with additional strokes, due to extensive shearing of the mechanically trapped aluminium, and could eventually cause galling.

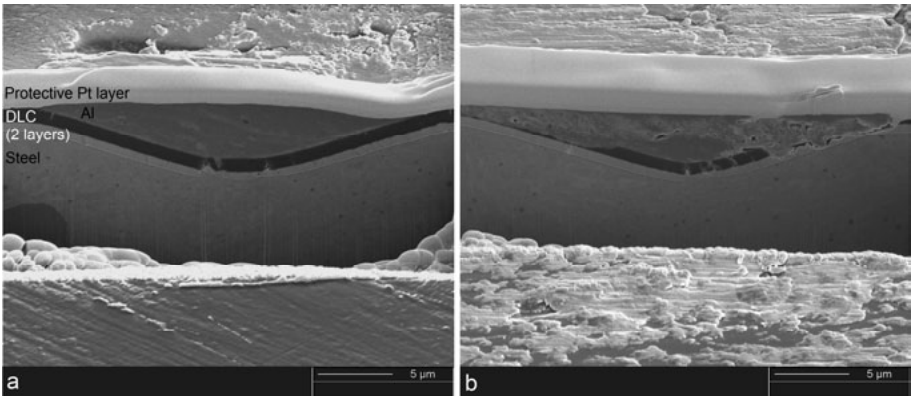

Figure 21. Cross-section images of indented tools after a) a single stroke (230 N) and b) multiple strokes (360 N).

Main conclusions

Occasional indents contribute to the initial transfer of aluminium. The transferred aluminium is mechanically trapped and hardened during subsequent sliding. This can lead to galling and deteriorate the surface finish of the formed products in production. However, the overall surface finish is decisive for the total friction and tool life, small scale damages with limited area coverage have no significant influence.

Galling initiation studies

Paper VI and VII

Aim

Surface roughness has shown to be of high importance when it comes to galling resistance. A rough surface causes immediate aluminium transfer while a smooth surface can withstand transfer for a longer sliding distance, as long as the chemistry is favourable. Occasional defects in such a coating cause immediate transfer, however no build-up. A friction coefficient that increases with sliding distance is still noted, due to transfer of work material to the polished coating. The aim with this study was to compare the

behaviour of a surface that causes galling to a galling resistant surface, on the microscopic level, to study galling initiation and the effect from tool surface roughness.

Experimental

Tests were performed in an in situ sliding rig in an SEM. Two tool materials were used; one cold work tool steel (grade C) and a galling resistant DLC coating (No. 3). Both materials were flat and used in fine polished condition (Ra < 0.05 μm) as well as fine polished with intentional scratches. The scratches were made by a single SiC grain and perpendicular to the sliding direction in the test. The work material was aluminium cylinders AA6082 with a conical end. The cones were made as sharp as possible, with a tip angle of about 35°, however with a flat end of about 50-100 μm in diameter. The diameter increased during loading and subsequent sliding, due to plastic deformation of the tip. The load used was 3 N and the sliding speed was 3 mm/min. The tests were performed unlubricated with 1, 5 and 10 passages in the same track, with both polished and intentionally scratched surfaces of both tool materials. Each passage resulted in a sliding length of 3 mm (against uncoated tool steel) to 4 mm (against DLC coated tool steel) for the work material, while the tool material experienced 100-200 μm sliding (the diameter in the sliding direction of the deformed tip).

Results and discussion

In the tests against polished uncoated tool steel flats the friction coefficient increased for every passage until a steady state level was reached, after about 6 passages, see Fig. 22a. With corresponding intentionally scratched surface, the scratches gave rise to high friction peaks, see Fig. 22b. However, the saturation level for the subsequent sliding, reached after about 3 passages, was at the same level as in the polished tests and slightly lower than the peaks. Tests with a polished DLC surface showed relatively low friction, and no influence from the number of passages in the same track, see Fig. 22c. Introduction of scratches to such a surface again led to high friction peaks and thereafter a slow decrease until the initial friction value was reached, see Fig. 22d. The sliding distance needed for the friction to go back to the initial value increased with each passage.

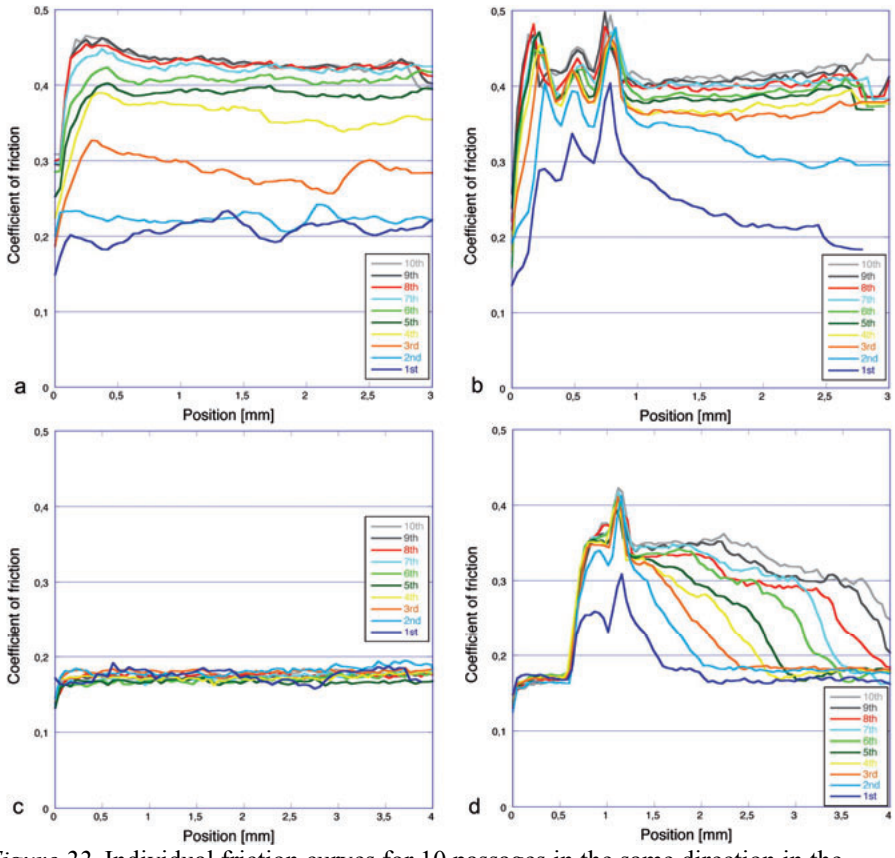

Figure 22. Individual friction curves for 10 passages in the same direction in the same track. Aluminium tip sliding over a) polished tool steel, b) polished tool steel with three intentional scratches, c) polished DLC and d) polished DLC with two intentional scratches.

The friction development is an indication of changes on the contacting surfaces during testing. The surfaces were closely studied in the SEM during and after testing.

Aluminium was immediately transferred to the polished tool steel surface during sliding. The area coverage increased with number of passages and covered a large area after 10 passages, see Fig. 23a. The transfer events were closely related to the positions of carbonitrides in the tool steel, while carbides were unaffected, see Fig 23b.

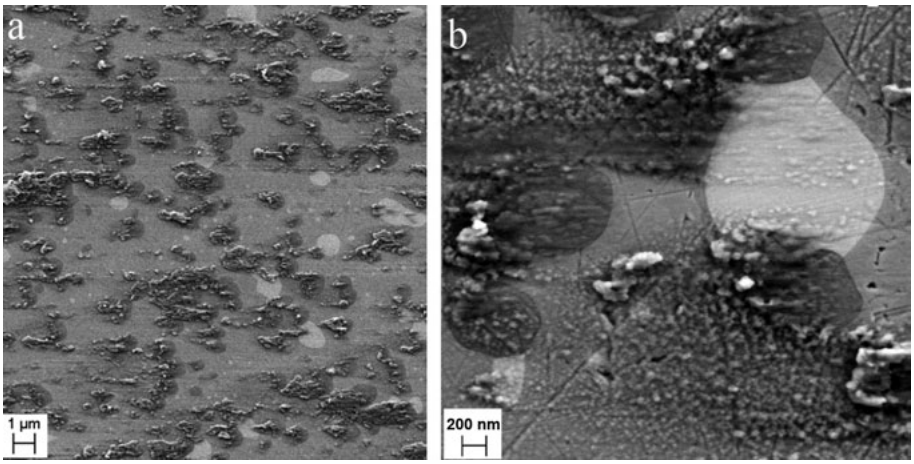

Figure 23. SEM images showing the tool steel after 10 passages in the same track. a) Overview and b) detail showing transferred aluminium mainly on the dark carbonitrides.

After sliding against DLC, no transferred aluminium was to be found in the contact track in general, see Fig. 24a. However, some aluminium was found transferred to sporadic defects in the surface, see Fig. 24b, but this was rare.

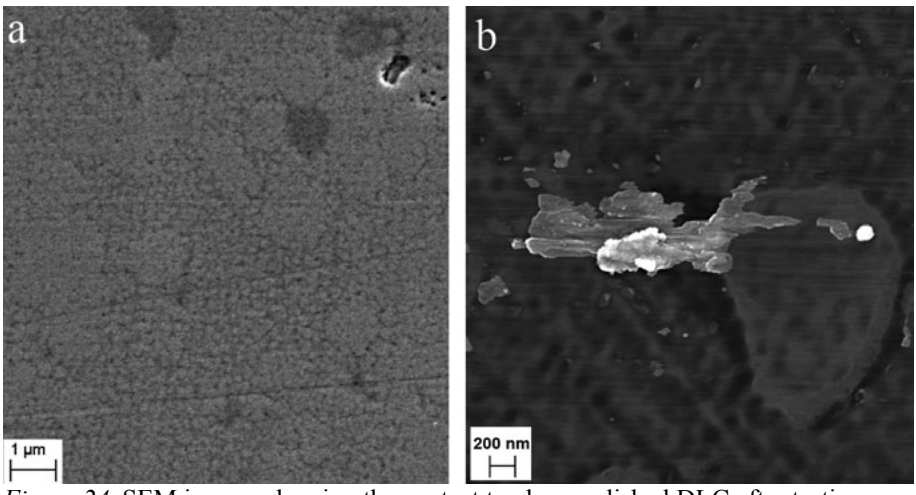

Figure 24. SEM images showing the contact track on polished DLC after testing. a) Overview and b) one rare transfer event connected to occasional surface defects.

The two tested tool materials obviously have different chemistry, but they also had different surface topography on the nanoscale, see Fig. 25. The tool steel showed rough carbonitrides protruding about 15 nm and smooth carbides protruding about 2 nm. The DLC surface was flat, with random irregularities protruding about 2 nm.

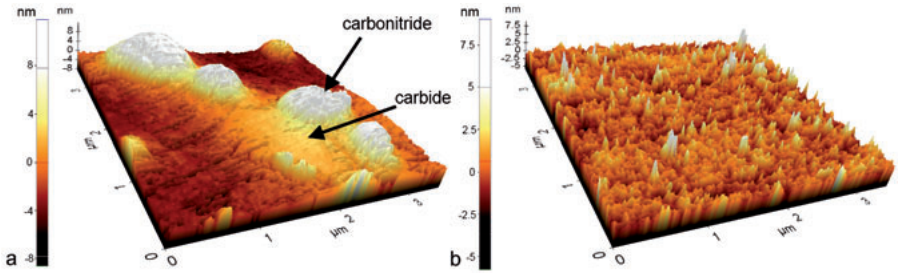

Figure 25. AFM images showing the topography of the polished tool materials before testing. Scanned area is 3.5 µm x 3.5 µm. The magnification in the Z-direction is exaggerated. a) Uncoated tool steel and b) DLC. Observe the difference in colour scale.

Introduction of scratches caused friction peaks correlated to the position of those. In case of DLC coating, the friction coefficient was influenced also during subsequent sliding against the polished surface. The scratches cause direct aluminium transfer to the scratches, but aluminium continued to be transferred also after passing the scratches, see Fig. 26. It was also observed that some transferred aluminium was relocated during continuous sliding, compare the 6^{th} and 7^{th} passage against DLC. Also worth noticing is that the aluminium adhered to the scratch in the tool steel build-up in front of the scratch. The build-up effect on the scratched DLC was less prominent.

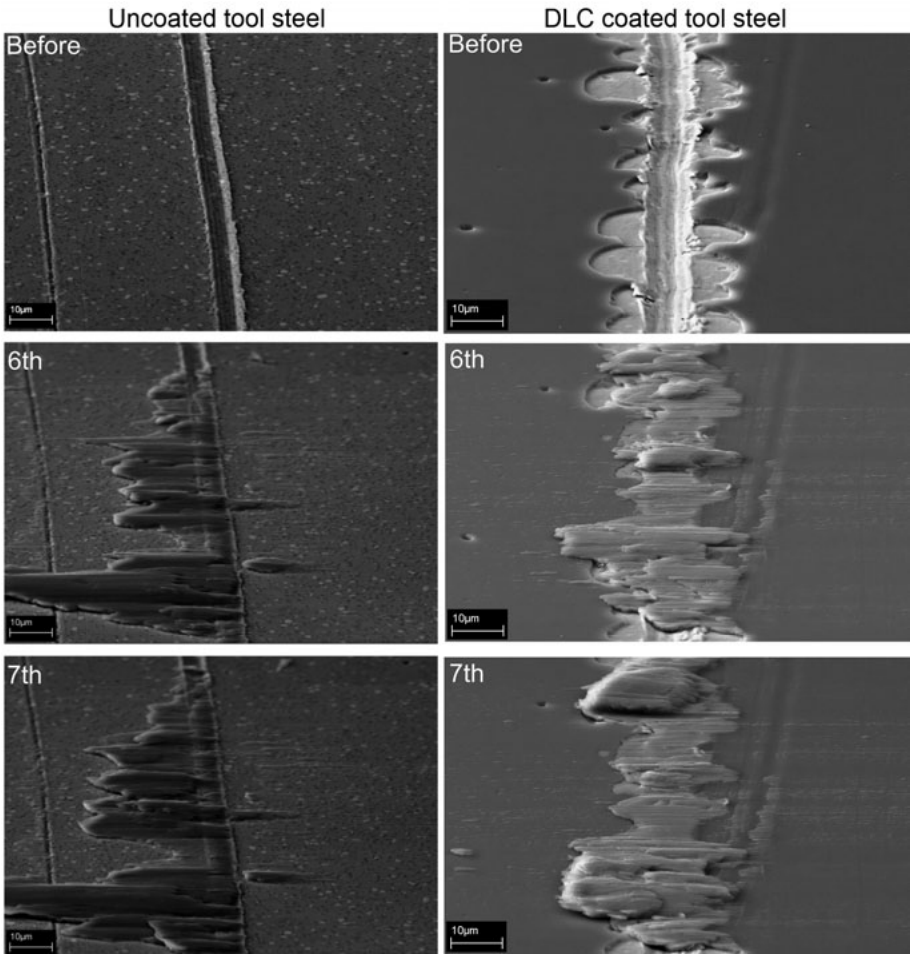

Figure 26. SEM images showing the last scratch from tests with the scratched surfaces as observed during the tests. Sliding direction of the aluminium pin was from left to right. Uncoated tool steel is shown to the left and DLC to the right.

Sliding against the polished uncoated tool steel surface resulted in approximately the same friction irrespective of former scratch passage or not. As the contact track showed the same appearance with the same extent of aluminium transfer, this is reasonable. With DLC on the other hand, the friction was significantly higher after passing a scratch and this was reflected when studying the contact tracks. Aluminium was now transferred to the polished surface and for longer and longer sliding distance per passage, reflected in the longer and longer time it took to get down to the initial friction coefficient. The extent and area coverage of the transfer increased with number of passages as well, see Fig. 27.

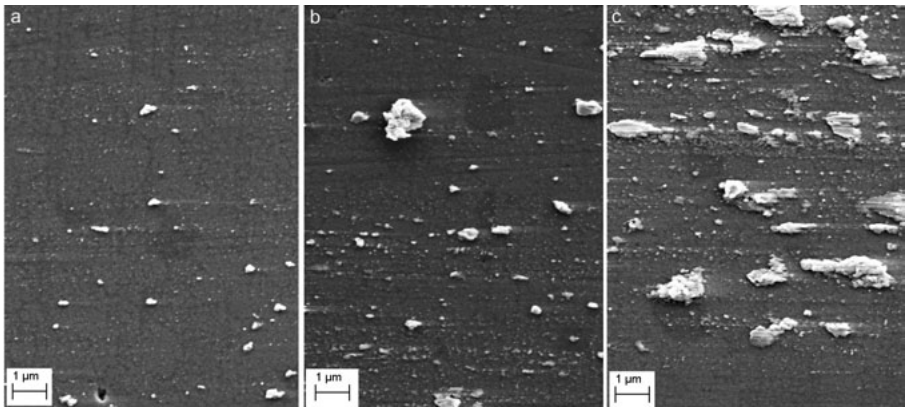

Figure 27. SEM images showing the DLC contact track 200 µm after passage of the last scratch. The amount of transferred aluminium increases with number of passages. a) 1 passage, b) 5 passages and c) 10 passages.

The passage of the scratches significantly changed the contact between DLC and aluminium. From being a stable contact without transfer events when no scratches were present, aluminium was now transferred to the fine polished surface.

The passage over the scratch severely damages the aluminium tip, resulting in an uneven sliding surface where the stable protective oxide is partly missing. This leads to subsequent transfer of aluminium to the DLC coating. However, the friction did decrease with the sliding distance after passage of the last scratch, and this is due to a healing effect of the aluminium work material. With the fine polished coating surface following the scratch passage, the aluminium tip can be smoothened in the contact. The low adhesion between the DLC and aluminium oxide, allowing transfer free sliding in the polished tests, facilitate reformation of a stable oxidised sliding surface. The aluminium is sheared in the sliding direction, from the front towards the end of the tip, while this smooth and very fine grained film is formed, see Fig. 28. When the sliding surface is smooth and the oxide separates the aluminium from the DLC coating, transfer is interrupted. In the next passage in the same track it takes some longer sliding distance to lower the friction, due to the aluminium lumps present in the track from earlier passages acting as irregularities breaking the oxide and aggravating the formation of a stable sliding surface.

Figure 28. SEM image of a cross-section in the aluminium tip surface showing the formation of the smooth protecting surface film, characterized by sub-micron sized, equiaxed grains. Sliding direction of the counter material is from left to right.

When sliding against the fine polished uncoated tool steel surface the small protruding carbonitrides cause stress concentrations and the aluminium surface is damaged. If reactive aluminium is exposed, it adheres to the carbonitrides and steel matrix, resulting in transfer. It is also possible that the adhesion between aluminium oxide and the steel matrix/carbonitrides is stronger, than that between aluminium oxide and DLC. This would also cause transfer. Irrespective of transfer mechanism, the formation of a smooth and stable sliding surface would be continuously disturbed and very limited healing effect would be permitted on the tool steel surface.

Main conclusions

Uncoated tool steel causes immediate transfer of aluminium, already after 100-200 µm of sliding (corresponding to single passage of the tip) or less. This is due to protruding carbonitrides breaking the aluminium oxide and causing transfer or high adhesion between aluminium and the tool steel matrix and/or the carbonitrides.

Finely polished DLC coated surfaces do not cause aluminium transfer unless the work material surface is damaged, since the surface roughness is too small to cause stress concentrations and break the aluminium oxide. If the aluminium oxide is broken, for example when passing a scratch, the reactive aluminium adheres to the DLC surface. However, the aluminium surface can be healed by continued sliding against the well polished DLC surface, forming a smooth and stable sliding surface. The transfer events stop until the oxide surface is damaged once again.

Contributions – on cutting

Verification of intermittent sliding test rig performance

Paper VIII

Aim

The aim was to design a suitable test equipment to reproduce transfer films found on milling tools. The demands on the new equipment were to accurately mimic the sliding between a chip and a rake face of a tool, to allow for cheap screening of materials, study of transfer mechanisms and an easy interpretation of results.

Experimental

A sliding contact rig was modified to work intermittently, to imitate the contact and sliding conditions of the rake face in milling. Testing was performed with intermittently loaded PVD TiN coated HSS cylinders against a rotating cylinder made from a case hardening steel. The transfer layers found on the test pieces were compared to those from single insert milling tests with PVD TiN coated inserts and work material from the same batch. The comparison was performed with respect to appearance and chemical composition, with the use of SEM, EDS and AES.

Results and discussion

The surface appearance of the contact tracks on the cylinders was similar in all repeated tests, with a dark transfer layer in the middle of the track surrounded by a light grey transfer layer, see Fig. 29. In the middle of the track the pressure is high, thus there is significant deformation of the work piece and the heat generation is most severe. In the surrounding area the pressure and temperature are lower, but there is still close contact between the work material and tool specimen.

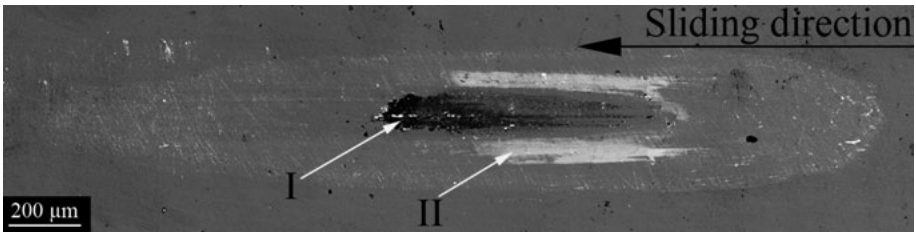

Figure 29. Contact track on the cylindrical test piece representing the rake face of a cutting tool. Imaged using SEM compositional mode, showing the two different areas, dark (I) and light grey (II), of adhered material. The sliding direction of the work material is indicated.

A comparison with the transfer films on real milling inserts after single insert milling showed similar areas of transferred material, see Fig. 30. The highest pressures and temperatures prevail close to the cutting edge, where the dark transfer layer was found. Around the edges, where the contact conditions were less severe, a light grey transferred layer was seen. The share of this layer was less than that found on the tool cylinders, but the area of high pressure was larger on the cutting insert.

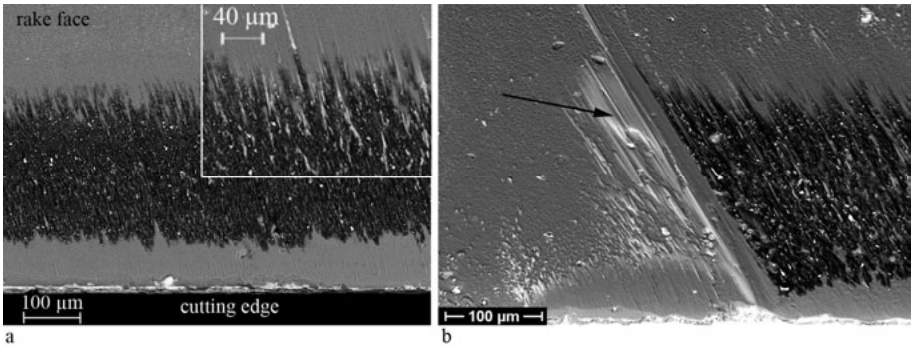

Figure 30. SEM images in compositional mode of a cutting insert after single tooth milling. a) Contact track with the two different transfer areas. The inserted picture is a magnification of the upper part of the image in order to clarify the presence of light grey transferred material in this region. The same type of adhered material was found at the rim of the chip/tool contact, indicated by an arrow in b).

Chemical analysis of the transfer layers with AES showed that the composition of the dark and light grey transfer layers, was very similar in the two test types, compare Figs. 31 and 32. The dark transfer layer consisted of accumulated alloying elements that were highly oxidised, while the light grey transfer layer consisted of oxidised steel.

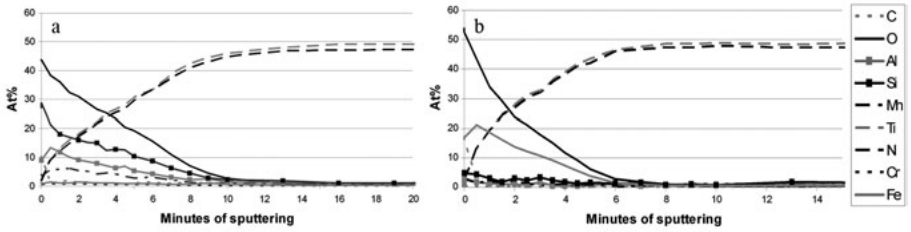

Figure 31. AES depth profile of a) the dark area and b) the bright area on a tool cylinder.

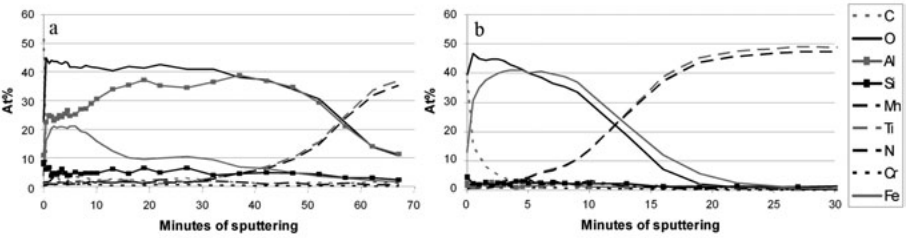

Figure 32. AES depth profile of a) the dark area and b) the bright area on a cutting insert.

Main conclusions

A sliding contact rig was modified to allow for intermittent sliding test. Two types of transferred material were found in the contact track after testing. The two types were similar in appearance and composition to those found on cutting inserts. Thus, the test is of high relevance, since it accurately imitates the material transfer in actual milling.

Transfer film formation

Paper IX and X

Aim

The aim was to characterize the transfer films formed in the intermittent sliding test and study the formation of the films. Increased knowledge about the transfer layer formation increases the possibility to design transfer layers with desired properties. Influence from tool surface finish was also considered.

Experimental

Intermittent sliding tests were performed with a PVD TiN coating on HSS substrate cylinders sliding against case hardening steel. The HSS substrate cylinders were prepared to three surface roughnesses before coating deposition. The finest polished surface was polished also after the coating

deposition, while the other two were used as deposited. The resulting surface roughnesses were; fine polished with Ra 0.06 µm, semi polished with Ra 0.2 µm and rough with Ra 0.3 µm. Testing was performed at moderate sliding speed, 120 m/min. The transfer layers found on the test pieces were analysed using SEM, EDS, AES and TEM.

Results and discussion

From the intermittent sliding tests two types of transfer films were identified. One dark transfer layer was found in the middle of the contact track, where the pressure and temperature became the highest, and the oxygen supply from the air was limited. A second transfer layer was found in the periphery of the contact track, where the pressure and temperature were lower and the oxygen supply higher. These two zones were separated by an intermediate zone, see Fig. 33.

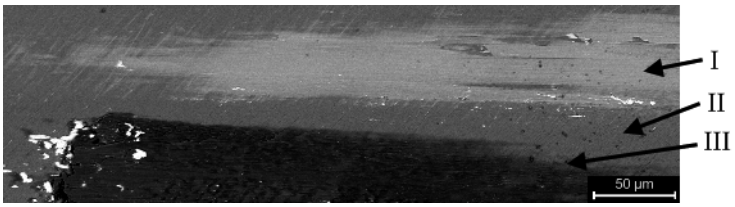

Figure 33. SEM image of part of the contact track on fine polished TiN showing two distinct zones of transferred material, light grey (I) and dark (III), separated by an intermediate zone (II). Sliding direction of the work material was from right to left.

In the intermediate area, SEM did not reveal any transfer layer on top of the coating, and neither did EDS analysis, see Fig. 34. However, the elemental contents of the dark and light grey transfer layers were analysed with EDS. The dark transfer layer mainly consisted of accumulated alloying elements from the work material, including aluminium, manganese and silicon, together with oxygen. This was also confirmed by the AES analysis in Fig. 31a. The light grey transfer film consisted of mainly iron oxide, however including small amounts of the alloying elements in the work material.

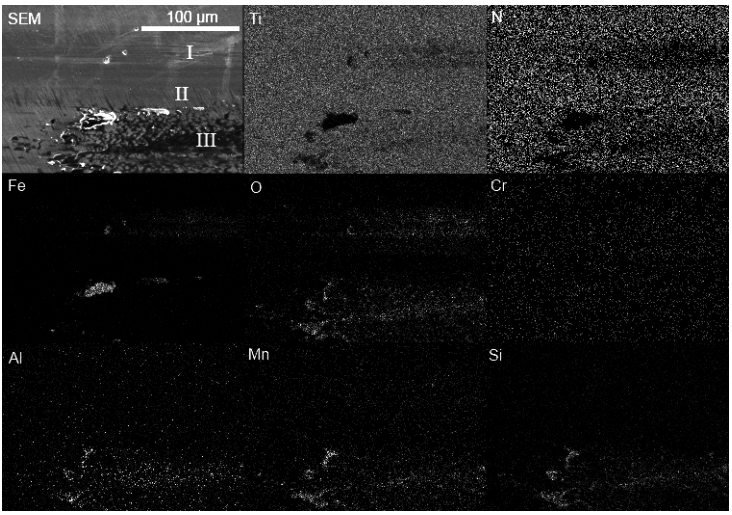

Figure 34. EDS analysis of part of the contact track on polished TiN after testing with moderate speed. Parts of the light grey (I) and dark (III) area are analysed, separated by intermediate area (II).

A more surface sensitive analysis was performed in the intermediate zone using AES, see Fig. 35. From this analysis it was evident that also this area had transferred material, while only a very thin layer. The composition of this transfer layer was a mixture between the two other transfer films, with mainly O, Si, Fe, Mn, Al and Cr. Some C was also detected, probably deriving from impurities adsorbed on the surface.

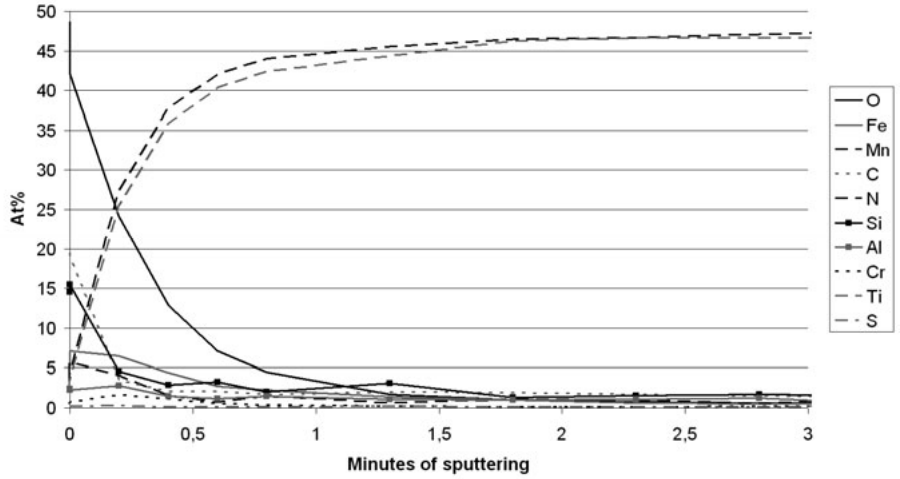

Figure 35. AES depth profile in the intermediate area on polished TiN.

To more closely analyse the transfer films, EFTEM studies were performed. In the dark transfer layer, crystalline Fe-rich particles were found in an

amorphous or nanocrystalline matrix of oxidised Al, Mn and Si, see Fig. 36. Additionally, a thin Fe layer was found in the interface between the transfer layer and the coating.

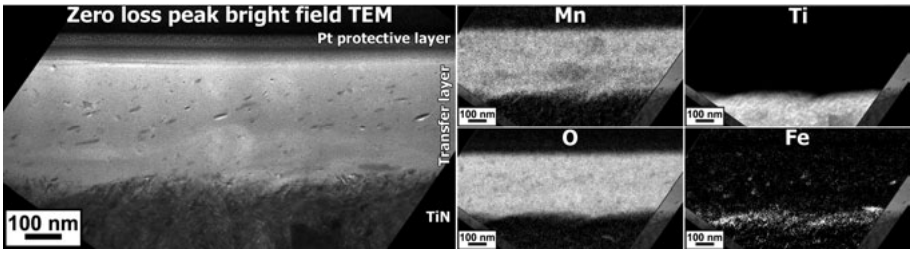

Figure 36. The dark transferred layer on polished TiN in cross-section, energy filtered TEM. The oxidised matrix is exemplified by Mn and O.

In the light grey transfer layer, crystalline iron oxide particles were found in a nanocrystalline matrix of iron oxide. Also here an interface layer with differing composition was found. It contained Cr and to a low extent also Mn. A Cr layer was also found closer to the upper surface, see Fig. 37.

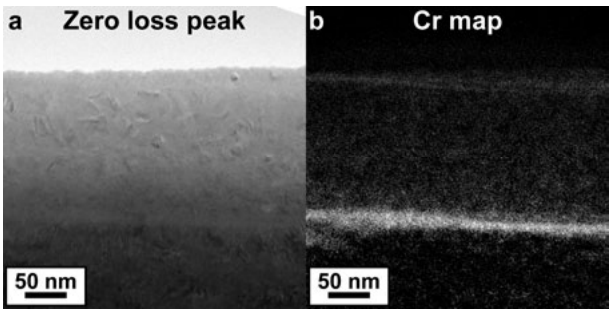

Figure 37. TEM images showing the light grey transferred layer on polished TiN. a) Bright field micrograph and b) energy filtered Cr-map.

When the rougher surfaces were used, the transfer film formation was less distinct and mainly connected to the grinding ridges. With the roughest sample, the work material was not just chemically transferred, but also abrasively worn.

Main conclusions

Two transfer layers are formed separately, one consisting of Mn, Si, Al and O with an intermediate layer of Fe and one consisting of Fe, Mn, Cr and O with an intermediate layer of Cr and Mn. An area with very limited transfer of work material separates the two transferred layers. If the coating surfaces are too rough, the transfer layers do not grow thick enough to separate the surfaces and the work material becomes abrasively worn.

Tool coating evaluation

Paper IX and X

Aim

The aim was to compare two commercial PVD tool coatings in terms of transfer film formation and performance. With a successful coating, the tendency for built-up edge is low and the cutting speed can be high without altering the machined surface and tool life.

Experimental

The PVD coatings included were TiN and AlCrN. Both were deposited on HSS cylinders and polished after deposition to Ra 0.06 μm. Testing was performed in intermittent sliding contact against ferrite pearlitic case hardening steel with three different speeds; low (60 m/min), moderate (120 m/min) and high (235 m/min). Each test comprised 50 engagements and the duration of each engagement was adjusted to give approximately the same sliding length per contact (0.05-0.09 m). Each test was repeated three times for statistical verification. Complementary tests with moderate speed were performed in intermittent sliding as well as continuous sliding with varying total sliding lengths; 4, 6, 10 and 20 m.

Results and discussion

The same type of transfer layers as described in the preceding section were identified on both types of coatings, when tested in intermittent contact with moderate speed. At low speed, another type of transfer was noted. Both types of coatings showed transferred lumps of work material, rather than a continuous film, see Fig. 38a. The transferred lumps were grain refined and probably harder than the original work material, see the cross-section through a lump in Fig. 38b. If they are hardened, the transferred lumps can scratch the work material and be compared to a build-up edge in cutting.

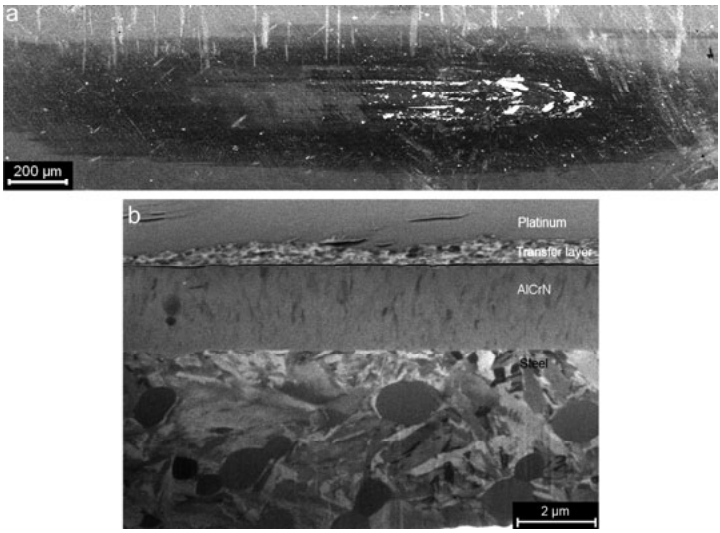

Figure 38. Images showing the AlCrN after intermittent contact with low speed. a) Top view imaged with SEM and b) cross-section through a transferred lump of work material imaged with ion beam. Note the fine grain structure in the transferred lump.

A comparison of the thickness of the transferred lumps showed that the lumps were generally thicker on TiN, up to 6 µm, compared with 3-4 µm on AlCrN, see Fig. 39.

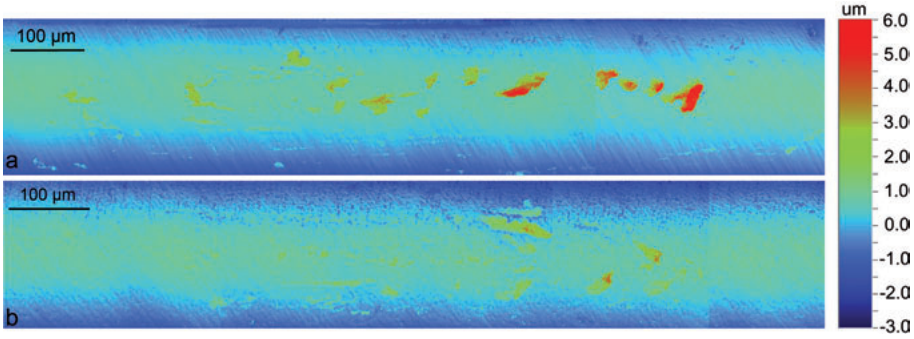

Figure 39. White light interference profilometry measurements showing the distribution and thickness of the transferred lumps in the contact track after testing with low sliding speed on a) TiN and b) AlCrN.

With high cutting speed, a third contact track appearance was observed on TiN. A large lump of material was noted in the middle of the contact track, see Fig. 40. The lump consisted mainly of Fe, with detectable amounts of the alloying elements Cr and Mn. In the rear end of the contact track, small amounts of the dark transfer layer were detected. Light grey transferred material was found where expected from earlier testing. AlCrN showed one

contact track with the same type of central lump, however much smaller. The other two contact tracks on AlCrN were similar to those after testing with moderate speed and missing the central lump.

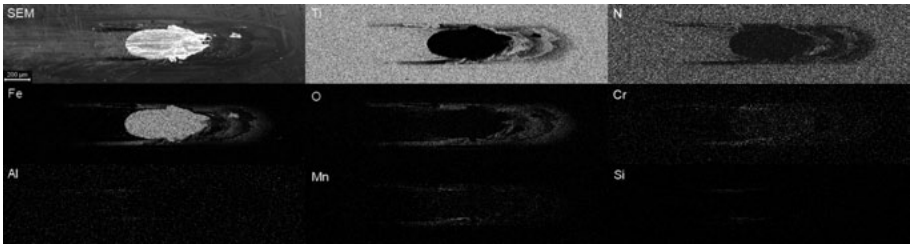

Figure 40. SEM image and compositional maps from EDS analysis of a contact track on TiN after testing with high sliding speed.

A cross-section revealed the cause of work material transfer, see Fig. 41. The increased heat generation in the contact, due to increased sliding speed, has caused softening of the substrate material. The HSS yields under the contact pressure, resulting in brittle coating fracture, removal of the coating and exposure of the softened HSS [11, 32, 43]. This leads to subsequent rapid wear. The AlCrN coating has high oxidation resistance and low thermal conductivity and performs well at the higher cutting speed [44]. A less intimate contact between transferred material and coating could also be an explanation, but has not yet been verified.

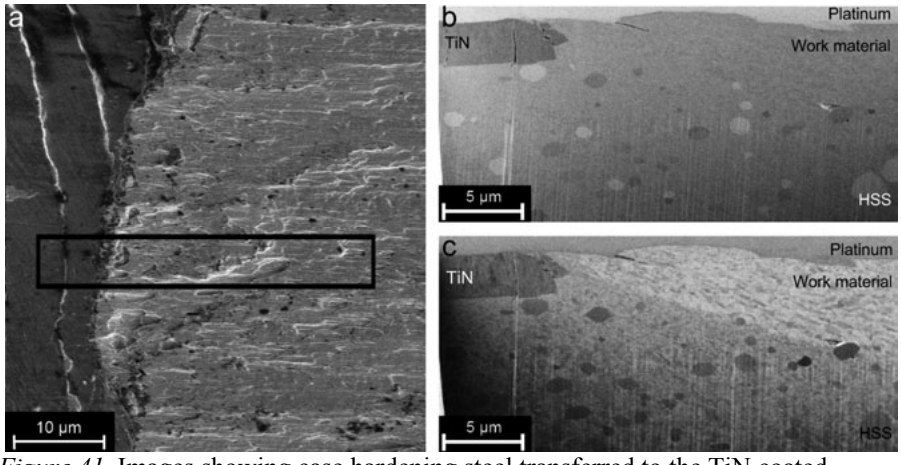

Figure 41. Images showing case hardening steel transferred to the TiN coated sample after testing with high sliding speed. The coating has fractured and been removed, and work material has filled the deep wear scar into the tool steel. a) Top view of the rear end of the lump (SEM, secondary electron contrast), b) cross-section (SEM, secondary electron contrast) and c) cross-section (same area) imaged using a focused ion beam. The area indicated in a) is the positioning of the cross-section imaged in b) and c).

To further investigate the performance, longer sliding tests were performed in intermittent as well as continuous contact with moderate sliding speed. The continuous contact tests do not allow for cooling of the tool samples, resulting in higher contact temperature. These tests showed that TiN was fractured already after 4 m sliding, both in intermittent and, even more severe, in continuous sliding, see Fig. 42. Contrastingly, AlCrN did not show any cracks even after 20 m of continuous contact sliding.

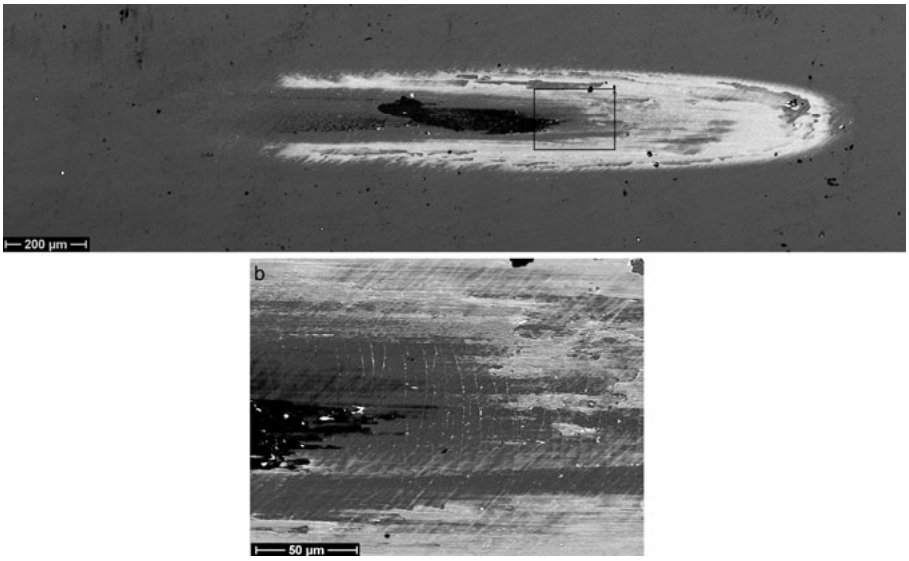

Figure 42. SEM imaging with backscattered electrons showing an example of the contact tracks on the TiN sample after sliding 4 m in continuous contact.
a) Overview and b) magnification of the area indicated in a).

Main conclusions

Too low sliding speed results in an uneven transfer of steel, similar to a built-up edge. Too high sliding speed, on the other hand results in thermal softening of the substrate, which leads to coating failure and flaking. Moderate sliding speed provides suitable conditions for forming the two types of transfer layers usually expected in milling, irrespective of coating type. AlCrN shows lower pick-up tendency at low speeds and provides better substrate protection at high speeds than TiN does. Increased sliding length as well as continuous sliding leads to fracture of the TiN coating. No such observations were made with AlCrN. AlCrN shows a superior high temperature performance compared with TiN.

Conclusions

The detailed properties of the surfaces have proven very important for transfer of work material to tools. The chemistry as well as surface roughness is decisive for the mechanism of transfer. The prevailing conditions in the contact also strongly influence the transfer film formation.

On forming

Rough tool surfaces can keep lubricant reservoirs in the scratches and pockets. The lubricant slows down the friction increase and reduce transfer, but is slowly transported out of the contact. The loss of lubricant is followed by friction increase and severe aluminium transfer. If unlubricated aluminium is used, transfer occurs immediately and the friction is high.

Polishing of the tool surfaces reduces the friction. If lubricant is used, the friction is relatively low and stabile. However, the lubricant becomes squeezed out from the contact due to high forming forces. This starvation of lubricant is followed by aluminium transfer. If the smooth surface has high adhesion to aluminium, the shear force is too high for the transferred aluminium to be removed. This results in aluminium staying on the surface and more aluminium being transferred to the initial transfer zones, followed by increasing friction, as with unlubricated tests.

If there is a suitable low adhesion coating on the tool piece, transfer of work material can be avoided. This is valid as long as there are no topographical defects on the surface, which act to break the oxide and activating the work material. However, there are small defects also in the best polished surfaces that will eventually activate the work material surface and cause transfer of aluminium. Aluminium is then transferred to the defect, but also to the fine polished surface, once it is activated. When transfer events have occurred, the process will escalate with the next pieces to be formed, due to secondary roughness. The surface becomes rougher with each forming cycle, due to more and more transferred fragments activating the work material. The transfer of aluminium escalates and a substantial friction increase is noted on the macroscopic scale.

The best recommendation for avoid galling is to use a galling resistant coating and to polish the tool surfaces as well as possible, avoiding large scale surface damage but also minimize the roughness on the nanoscale.

On cutting

The composition of the transferred material differs with the prevailing contact conditions. If the surfaces are rough, the work material is abrasively worn and transferred mainly as steel. With smooth surfaces other mechanisms become dominant. Low speed causes work material adhesion and chunks of work material is transferred to the tool. These transferred particles can be work hardened and deteriorate the surface finish of the piece. High speeds cause high heat generation and thermal softening of the tool substrate, which leads to coating failure and extensive wear of the tool. At moderate speeds two transfer film types are formed, depending on the pressure and temperature in the contact. The two transfer films formed at moderate sliding speed consists of Mn, Si, Al and O, with an intermediate layer of Fe, and Fe, Mn, Cr and O, with an intermediate layer of Cr and Mn, respectively. These films are desired since they are known to provide a stable cutting behaviour resulting in a predictable tool wear and a sufficient surface finish of the piece. The speed interval for each of these mechanisms depends, among other things, on the tool coating.

Sammanfattning på svenska (Summary in Swedish)

Om överföring av arbetsmaterial till verktyg

Bulkformning och skärande bearbetning är viktiga processer för att forma metaller inom industriell produktion. Vid bulkformning börjar man med ett ämne av arbetsmaterial, som sedan formas till önskad geometri i ett eller flera steg. Ett exempel på en bulkformningsprocess visas i figur 43, där ett flerdelat verktyg används; en övre stämpel, en undre stämpel och en dyna. Ämnet placeras i verktyget och deformeras sedan plastiskt av ett högt presstryck. Arbetsmaterialet tvingas fylla ut och anta formen av utrymmet som definieras av verktygsdelarna. Bulkformning karaktäriseras av stora spänningar, omfattande plastisk deformation och stora ytexpansioner.

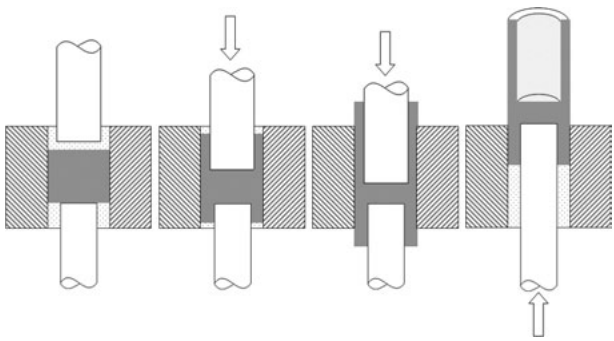

Figur 43. Skiss som visar ett exempel på en bulkformningsprocess, från ämne till färdig produkt.

I skärande bearbetning används verktyg med en eller flera skärande eggar som avverkar material från arbetsmaterialet för att få fram önskad geometri. Skäreggen tränger in i materialet och bildar en spåna, vilken glider över spånsidan på verktyget, se figur 44. Det bearbetade arbetsmaterialet passerar släppningssidan på verktyget. Skärande bearbetning kännetecknas av höga hastigheter, höga tryck och höga temperaturer.

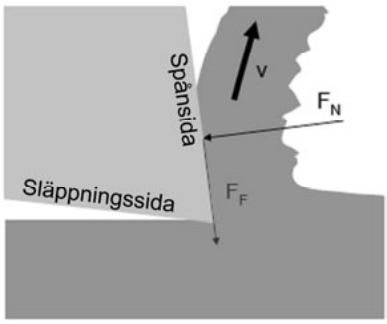

Figur 44. Skiss som visar ett exempel på en skärprocess, där arbetsmaterial avverkas från ämnet genom spånbildning.

De förhållanden som råder under de båda tillverkningsprocesserna leder ofta till att arbetsmaterial fastnar på verktygsytorna och förs över till verktygen. Vid bulkformning är detta ett omfattande problem. Det överförda arbetsmaterialet härdas i den tribologiska kontakten och blir hårdare än arbetsmaterialet i ämnet. Detta leder till att det överförda materialet kan repa produkten vid nästa formningsoperation. Fenomenet, som betecknas galling, leder i sin tur till hög friktion, höga presskrafter, försämrad ytfinhet hos de formade produkterna och betydande svårigheter att producera komplicerade geometrier. Produktionen måste då avbrytas för rengöring eller utbyte av verktyget, vilket är mycket kostsamt för industrin.

Vid skärande bearbetning kan det vara önskvärt att få en film av överfört arbetsmaterial på verktygsytan. Filmen kan skydda spånsidan mot värme och nötning och bidra till låg friktion. Dock måste den överförda filmen vara av rätt typ och ha rätt sammansättning för att ge ett stabilt och förutsägbart beteende i drift. Om filmen istället är av fel sort kan det leda till sämre ytfinhet hos produkten, stora problem i tillverkningsprocessen och i värsta fall bidra till att verktyget går sönder. Även här leder dålig kontroll av vad som händer på verktygsytan till oplanerade driftsstopp och höga kostnader, både för verktyg och för produktionsbortfall.

I den här avhandlingen har inverkan av verktygsmaterial och ytfinhet på överföringen av arbetsmaterial studerats för båda tillverkningsprocesserna. Detta har skett med hjälp av förenklade laboratorieutrustningar, som isolerar problemet, följt av omfattande ytstudier. Utvärderingen har omfattat tendens till överföring av arbetsmaterial, det överförda materialets fördelning, form och struktur samt dess kemiska sammansättning. Resultaten har sedan jämförts med exempel hämtade från verklig produktion, för att säkerställa att rätt mekanismer efterliknas.

Aluminium är ett vanligt arbetsmaterial vid bulkformning och det material som studerats i den här avhandlingen. Vid aluminiumformning uppstår problemen med materialöverföring när dålig smörjning infinner sig, t.ex. på grund av höga tryck eller stora ytexpansioner, då smörjmedlet inte

räcker till eller smörjmedelsfilmen brister. För att undvika att aluminium fastnar på verktyget kan det beläggas med en ytbeläggning av lämplig sammansättning, t.ex. ett skikt av diamantlikt kol (DLC). Dock måste ytbeläggningen vara mycket slät, även i nanoskala, för att bidra med sin fulla potential. Om det finns ojämnheter i ytbeläggningen kan dessa aktivera aluminiumet, genom att skada den skyddande ytoxiden på aluminium och ge höga spänningskoncentrationer. Aktiveringen gör att aluminium fastnar på verktyget, trots ytbeläggningens goda egenskaper att motstå galling.

Vid skärande bearbetning kan man erhålla den önskade filmen av arbetsmaterial genom att välja rätt skärdata. Geometrin och arbetsmaterialet är ofta bestämt av vilken komponent som ska produceras, vilket ger de generella förutsättningarna för skärprocessen, men även t.ex. skärhastigheten är avgörande för överföring av material till verktygsytan. Om en för låg skärhastighet används förs arbetsmaterialet över i klumpar och med en för hög hastighet blir verktyget för varmt och nötningen blir omfattande. Båda dessa mekanismer ger en instabil skärprocess. När en lämplig hastighet används fås tunna skikt av oxiderat arbetsmaterial, med en sammansättning som beror på förhållandena i kontakten. Dessa skikt ger ett stabilt skärförlopp. I vilket hastighetsintervall de olika mekanismerna uppträder beror delvis på verktyget och dess ytbeläggning, då de flesta skärverktyg är ytbelagda för att klara förhållandena i en skärprocess.

Acknowledgements

Ett stort tack till alla som har bidragit och satt guldkant på mina år som doktorand. Ett extra tack vill jag ge till

Staffan, för att du lärde mig vad tribologi är och för att du fick mig att fastna. Tack för all tid, all hjälp och ditt engagemang.

Urban, för att du visade mig en helt ny tribologi-värld och för att du tar dig tid, om det så är mitt i natten.

Mikael, för ett bra samarbete under ett roligt och intressant forskningsår.

Julia, för ett trevligt samarbete i labbet, med artikelskrivandet och för att du har svar på alla kugg-frågor.

Åsa och Sture, för att ni alltid har tid och engagemang när man kommer med frågor och funderingar.

Tor Erik, Inge, Cato och Sverre, för möjligheten att få jobba med ett intressant projekt, för ett bra samarbete och för att ni hjälpt mig att få inblick i aluminiumformningsvärlden.

Janne, Fredric och Victoria, för support och hjälp i och utanför renrummet.

Bagge, för din hjälp med alla oförståeliga datorproblem.

Anja och Karin, för att ni skött administrationen och hållit ordning på avdelningen.

Frida, Maria, Martina, Harald, Benny, Johanna, Petra, Peter och Fredrik, för all hjälp med stort och smått, men inte minst för trevligt sällskap i labbet, på avdelningen och på alla roliga resor vi varit på.

Avdelningsgänget under åren, för alla trevliga timmar i fika-soffan med vindlande associationsövningar och ”intressanta” samtalsämnen.

Min familj, för att ni alltid finns där och stöttar mig.

Mattias, för din kärlek, ditt tålamod och för att du alltid finns vid min sida!

References

1. R. D. Arnell, P. B. Davies, J. Halling, T. L. Whomes, *Tribology – Principles and Design Applications*, 1st ed., Springer-Verlag, NY, 1991
2. S. R. Schmid, R. D. Wilson, *Tribology in manufacturing*, in: B. Bhushan (Ed.), Modern Tribology Handbook, CRC Press, NY, 2001
3. N. Bay, *The state of the art in cold forging lubrication*, J. Mater. Process. Technol., **46** (1994) 19-40
4. N. Bay, M. Eriksen, X. Tan, O. Wibom, *A friction model for cold forging of aluminum, steel and stainless steel provided with conversion coating and solid film lubricant*, CIRP Ann. Manuf. Technol., **60** (2011) 303–306
5. R. P. Garrett, J. Lin, T. A. Dean, *An investigation of the effects of solution heat treatment on mechanical properties for AA6xxx alloys: experimentation and modeling*, Int. J. Plasticity, **21** (2005) 1640-1657
6. K. Lange, *Handbook of Metal Forming*, McGraw-Hill, NY, 1985
7. B. Podgornik, S. Hogmark, J. Pezdirnik, *Comparison between different test methods for evaluation of galling properties of surface engineered tool surfaces*, Wear, **257** (2004) 843-851
8. E. Schedin, *Galling mechanisms in sheet forming operations*, Wear, **179** (1994) 123-128
9. L. E. ST. Pierre, R. S. Owens, R. V. Klint, *Chemical effects in the boundary lubrication of aluminum*, Wear, **9** (1966) 160-168
10. C. Iliescu, *Cold-Pressing Technology*, Elsevier Science Publishing Company, Amsterdam, 1990
11. E. M. Trent, P. K. Wright, *Metal Cutting*, 4th ed., Butterworth-Heinemann, Oxford, 2000
12. *Skärteknik*, Ord & Form, Kristianstad, 1995 (In Swedish)
13. J. R. Davis, *ASM Specialty Handbook: Aluminum and Aluminum Alloys*, ASM International, OH, 1993
14. M. Mozetic, A. Zalar, U. Cvelbar, D. Babic, *AES characterization of thin oxide films growing on Al foil during oxygen plasma treatment*, Surf. Interface Anal., **36** (2004) 986–988
15. C. Ullner, A. Germak, H. LeDoussal, R. Morrell, T. Reich, W. Vandermeulen, *Hardness testing on advanced technical ceramics*, J. Eur. Ceram. Soc., **21** (2001) 439-451

16. A. K. Gupta, D. J. Lloyd, S. A. Court, *Precipitation hardening in Al-Mg-Si alloys with and without excess Si*, Mater. Sci. Eng., A **316** (2001) 11-17
17. G. Mrówka-Nowotnik, J. Sieniawski, *Influence of heat treatment on the microstructure and mechanical properties of 6005 and 6082 aluminium alloys,* J. Mater. Process. Technol., **162-163** (2005) 367-372
18. Y. Birol, *The effect of processing and Mn content on the T5 and T6 properties of AA6082 profiles*, J. Mater. Process. Technol., **173** (2006) 84-91
19. K. Mills, *Metals Handbook vol 9: Metallography and microstructures*, 9th ed., ASM International, OH, 1985
20. W. H. Cubberly, *Metals Handbook vol 1: Properties and selection: Irons and Steels*, 9th ed., ASM International, OH, 1985
21. G. Roberts, G. Krauss, R. Kennedy, *Tool Steels*, 5th ed., ASM International, OH, 1998
22. G. Krauss, *Steels: Processing, Structure and Performance*, ASM International, OH, 2007
23. K. Holmberg, A. Matthews, *Coatings Tribology*, 2nd ed., Elsevier, Amsterdam, 2009
24. S. Hogmark, S. Jacobson, M. Larsson, U. Wiklund, *Mechanical and tribological requirements and evaluation of coating composites*, in: B. Bhushan (Ed.), Modern Tribology Handbook, CRC Press, NY, 2001
25. B. Podgornik, S. Hogmark, O. Sandberg, *Influence of surface roughness and coating type on the galling properties of coated forming tool steel*, Surf. Coat. Technol., **184** (2004) 338-348
26. J. Robertson, *Diamond-like amorphous carbon*, Mater. Sci. Eng., R **37** (2002) 129-281
27. R. Hauert, *An overview on the tribological behavior of diamond-like carbon in technical and medical applications*, Trib. Int., **37** (2004) 991-1003
28. S. Hogmark, S. Jacobson, O. Wänstrand, *A new universal test for tribological evaluation*, Proceedings of the 21st IRG-OECD meeting in Amsterdam, D. J. Schipper (Ed.), 1999
29. S. Hogmark, S. Jacobson, O. Wänstrand, *The Uppsala Loadscanner – an Update*, Proceedings of the 22nd IRG-OECD meeting in Cambridge, D. J. Schipper (Ed.), 2000
30. M. Hanson, *On adhesion and galling in metal forming*, Ph.D. Thesis, Uppsala University, Uppsala, 2008
31. P. Hedenqvist, S. Söderberg, M. Olsson, S. Jacobson, *Failure mode analysis of TiN-coated High Speed Steel: In-situ scratch adhesion testing in the SEM*, Surf. Coat. Technol., **41** (1990) 31-49
32. P. Hedenqvist, M. Olsson, S. Söderberg, *Influence of TiN coating on wear of high speed steel tools as studied by new laboratory wear test*, Surf. Eng., **5** (1989) 141-150

33. J. I. Goldstein, D. E. Newbury, P. Echlin, D. C. Joy, C. Fiori, E. Lifshin, *Scanning Electron Microscopy and X-Ray Microanalysis*, Plenum Press, NY, 1981
34. L. A. Giannuzzi, F. A. Stevie, *Introduction to Focused Ion Beams*, Springer, USA, 2005
35. D. B. Williams, C. B. Carter, *Transmission Electron Microscopy*, Plenum Press, NY, 1996
36. P. van der Heide, *X-ray Photoelectron Spectroscopy*, John Wiley & Sons, New Jersey, 2012
37. H. J. Mathieu, *Auger Electron Microscopy*, in: J. C. Vickerman, I. S. Gilmore (Eds.), Surface Analysis: The principal Techniques, 2nd ed., John Wiley & Sons, Chichester, 2009
38. G. W. Stachowiak, A. W. Batchelor, G. B. Stachowiak, *Experimental methods in tribology*, Elsevier, Amsterdam, 2004
39. P. Eaton, P. West, *Atomic Force Microscopy*, Oxford University Press, NY, 2010
40. W. C. Oliver, G. M. Pharr, *An improved technique for determining hardness and elastic modulus using load and displacement sensing indentation experiments*, J. Mater. Res., **7** (1992) 1564-1583
41. B. Podgornik, S. Hogmark, *Surface modification to improve friction and galling properties of forming tools*, J. Mater. Process. Technol., **174** (2006) 334–341
42. B. Podgornik, J. Jerina, *Surface topography effect on galling resistance of coated and uncoated tool steel*, Surf. Coat. Technol., (2011) doi:10.1016/j.surfcoat.2011.11.041
43. S. Hogmark, M. Olsson, *Wear Mechanisms of HSS Cutting Tools*, SME Technical Paper, (2005) 1–14
44. W. Kalss, A. Reiter, V. Derflinger, C. Gey, J. L. Endrino, *Modern coatings in high performance cutting applications*, Int. J. Refract. Met. Hard Mater., **24** (2006) 399–404

Acta Universitatis Upsaliensis

Digital Comprehensive Summaries of Uppsala Dissertations from the Faculty of Science and Technology 894

Editor: The Dean of the Faculty of Science and Technology

A doctoral dissertation from the Faculty of Science and Technology, Uppsala University, is usually a summary of a number of papers. A few copies of the complete dissertation are kept at major Swedish research libraries, while the summary alone is distributed internationally through the series Digital Comprehensive Summaries of Uppsala Dissertations from the Faculty of Science and Technology.

Distribution: publications.uu.se
urn:nbn:se:uu:diva-165828

ACTA
UNIVERSITATIS
UPSALIENSIS
UPPSALA
2012